

# Heterogeneous Catalysis

## 5.1 | Introduction

*Catalysis* is a term coined by Baron J. J. Berzelius in 1835 to describe the property of substances that facilitate chemical reactions without being consumed in them. A broad definition of catalysis also allows for materials that slow the rate of a reaction. Whereas catalysts can greatly affect the rate of a reaction, the equilibrium composition of reactants and products is still determined solely by thermodynamics. *Heterogeneous* catalysts are distinguished from *homogeneous* catalysts by the different phases present during reaction. Homogeneous catalysts are present in the same phase as reactants and products, usually liquid, while heterogeneous catalysts are present in a different phase, usually solid. The main advantage of using a heterogeneous catalyst is the relative ease of catalyst separation from the product stream that aids in the creation of continuous chemical processes. Additionally, heterogeneous catalysts are typically more tolerant of extreme operating conditions than their homogeneous analogues.

A heterogeneous catalytic reaction involves adsorption of reactants from a fluid phase onto a solid surface, surface reaction of adsorbed species, and desorption of products into the fluid phase. Clearly, the presence of a catalyst provides an alternative sequence of elementary steps to accomplish the desired chemical reaction from that in its absence. If the energy barriers of the catalytic path are much lower than the barrier(s) of the noncatalytic path, significant enhancements in the reaction rate can be realized by use of a catalyst. This concept has already been introduced in the previous chapter with regard to the Cl catalyzed decomposition of ozone (Figure 4.1.2) and enzyme-catalyzed conversion of substrate (Figure 4.2.4). A similar reaction profile can be constructed with a heterogeneous catalytic reaction.

For example, G. Ertl (*Catalysis: Science and Technology*, J. R. Anderson and M. Boudart, Eds., vol. 4, Springer-Verlag, Berlin, 1983, p. 245) proposed the thermochemical kinetic profile depicted in Figure 5.1.1 for the platinum-catalyzed oxidation of carbon monoxide according to the overall reaction  $\text{CO} + \frac{1}{2} \text{O}_2 \rightleftharpoons \text{CO}_2$ . The first step in the profile represents the adsorption of carbon monoxide and

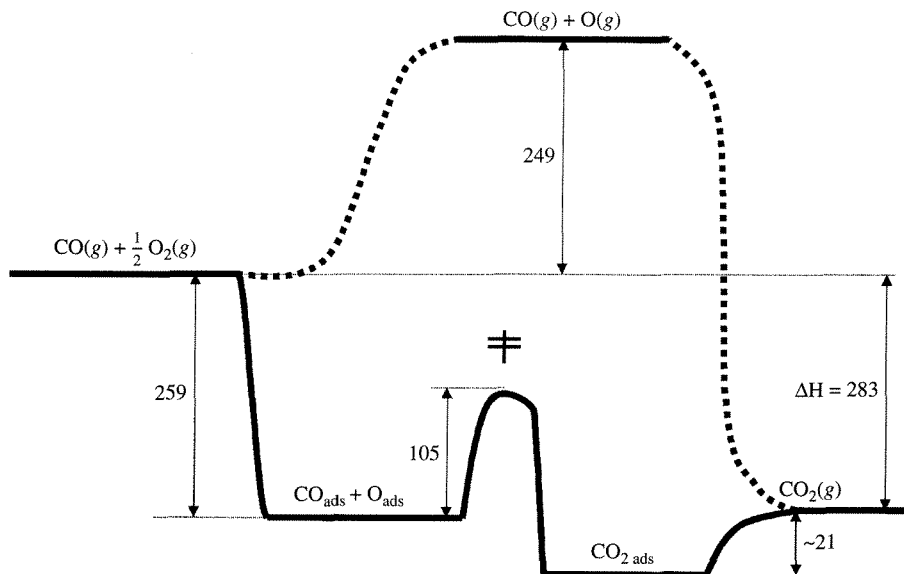


**Figure 5.1.1 |**

Schematic energy diagram for the oxidation of CO and a Pt catalyst. (From data presented by G. Ertl in *Catalysis: Science and Technology*, J. R. Anderson and M. Boudart, Eds., vol. 4, Springer-Verlag, Berlin, 1983, p. 245.) All energies are given in  $\text{kJ mol}^{-1}$ . For comparison, the heavy dashed lines show a noncatalytic route.

dioxygen onto the catalyst. In this case, adsorption of dioxygen involves dissociation into individual oxygen atoms on the Pt surface. The product is formed by addition of an adsorbed oxygen atom ( $\text{O}_{\text{ads}}$ ) to an adsorbed carbon monoxide molecule ( $\text{CO}_{\text{ads}}$ ). The final step in the catalytic reaction is desorption of adsorbed carbon dioxide ( $\text{CO}_{2\text{ads}}$ ) into the gas phase. The Pt catalyst facilitates the reaction by providing a low energy path to dissociate dioxygen and form the product. The noncatalytic route depicted in Figure 5.1.1 is extremely slow at normal temperatures due to the stability of dioxygen molecules.

### VIGNETTE 5.1.1

Perhaps one of the greatest triumphs of modern surface science is that rates of catalytic reactions on supported, transition metal particles can often be reproduced on very well-defined single crystal surfaces. The ability to reliably interrogate catalytic chemistry on single crystals allows for methodical exploration of the influence of atomic structure on catalytic activity [C. M. Friend, *Scientific American*, **268** (1993) 74]. Single crystals can be cut and processed to expose various low energy surface planes having specific atomic configurations. These various arrangements of surface atoms can be understood from the periodic nature of three-dimensional crystals. The three crystal structures of transition metals relevant to catalysis are called face-centered cubic, body-centered cubic, and hexagonal (see Figure 5.1.2).

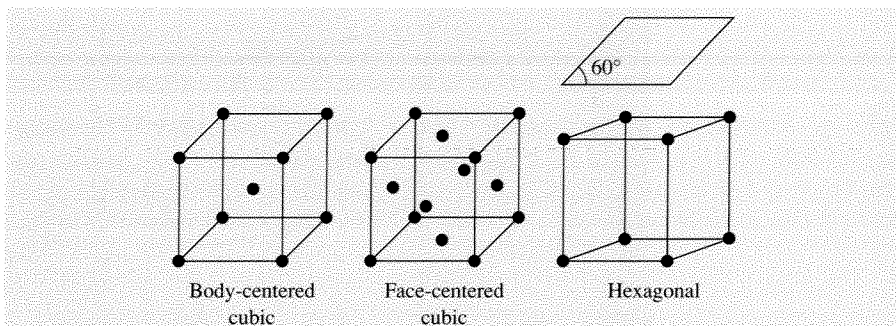


**Figure 5.1.2** | Crystal structures of catalytically relevant transition metals.

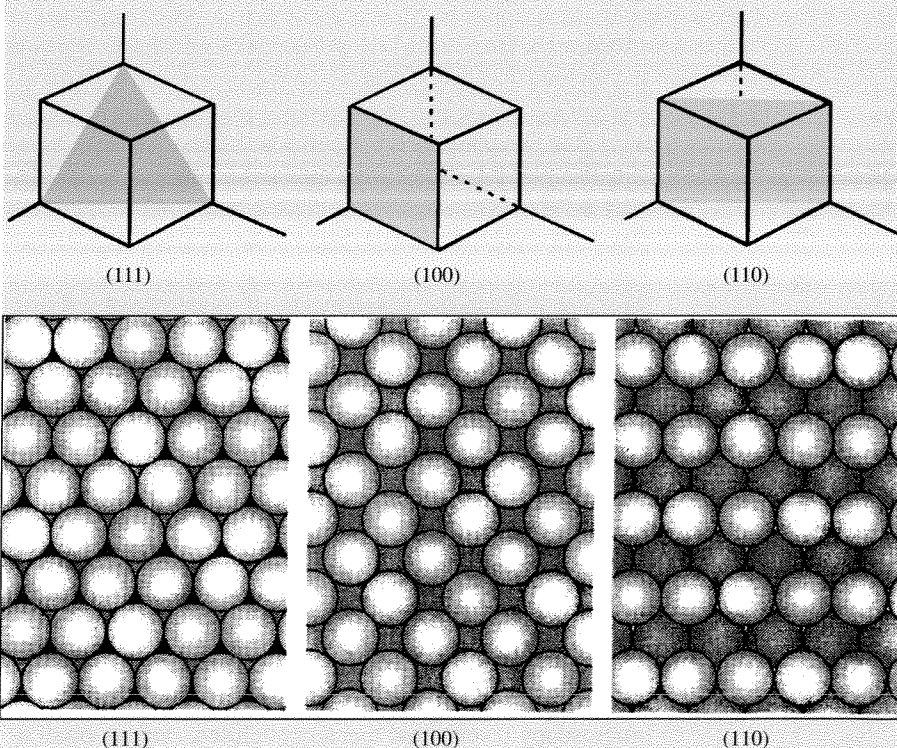


**Figure 5.1.3** | Atomic arrangements of the low-index surface planes of an FCC crystal. (Adapted from R. Masel, *Principles of Adsorption and Reaction on Solid Surfaces*, Wiley, New York, copyright © 1996, p. 38, by permission of John Wiley & Sons, Inc.)

Single crystal surfaces are associated with planes in the unit cells pictured in Figure 5.1.2 and are denoted by indices related to the unit cell parameters. Several examples of various low-index surface planes are shown in Figure 5.1.3 for the face-centered cubic structure.

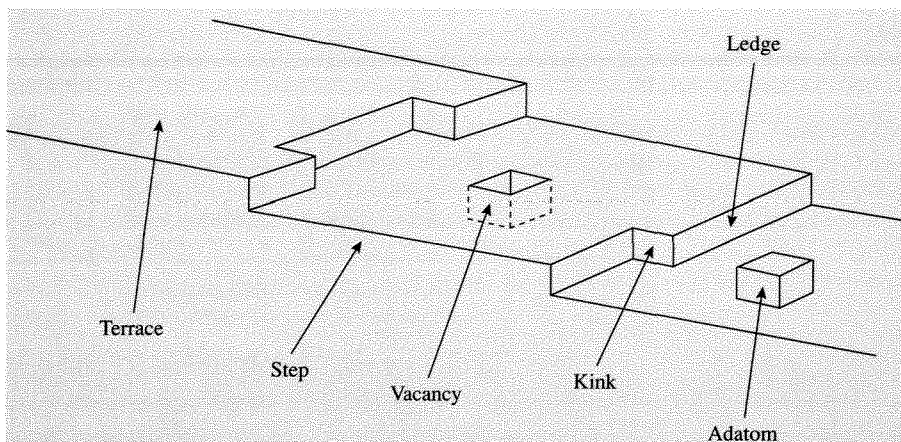
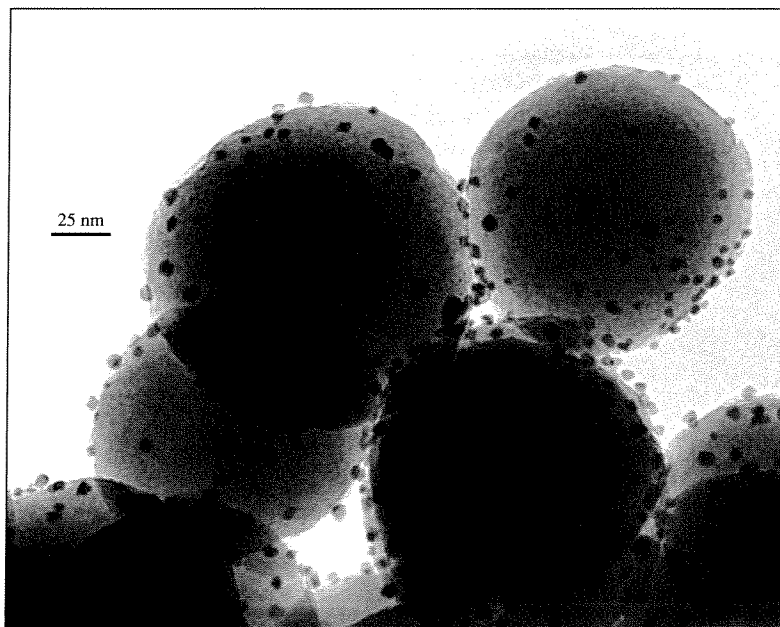


**Figure 5.1.4** | Schematic representation of a single crystal surface.

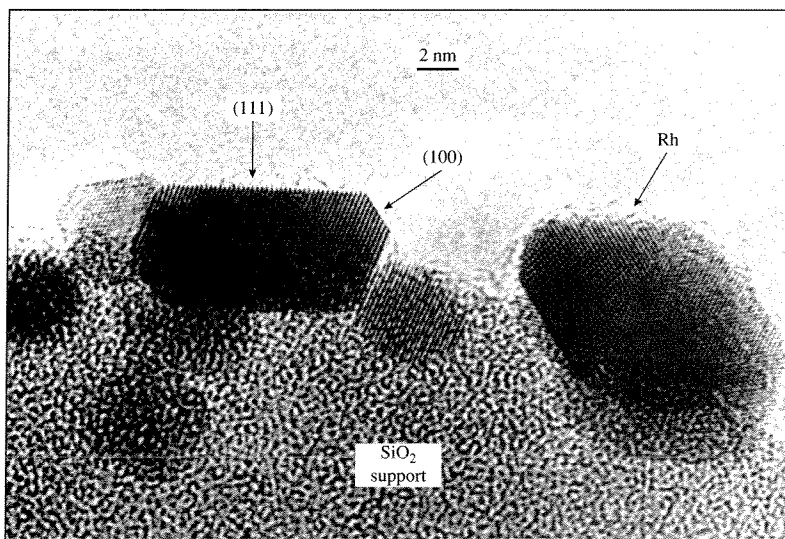
On real, single crystal surfaces, atomic positions associated with ideal surface planes are perturbed by relaxation effects and the presence of atomic-scale defects. It is, therefore, more correct to think of single crystal surfaces being composed of terraces of stable planes separated by atomic-scale steps or ledges that may have kinks. In addition, various point defects like atomic vacancies or surface adatoms may be present. A schematic representation of single crystal surfaces is shown in Figure 5.1.4. Interestingly, the number density of surface atoms in the stable planes of transition metals is about  $10^{15} \text{ cm}^{-2}$ , regardless of crystal face. This value of surface atom density is a good starting point for estimating the total number of adsorption sites or active sites on metal surfaces.

Since the number of atoms on the surface of a bulk metal or metal oxide is extremely small compared to the number of atoms in the interior, bulk materials are often too costly to use in a catalytic process. One way to increase the effective surface area of a valuable catalytic material like a transition metal is to disperse it on a support. Figure 5.1.5 illustrates how Rh metal appears when it is supported as nanometer size crystallites on a silica carrier. High-resolution transmission electron microscopy reveals that metal crystallites, even as small as 10 nm, often expose the common low-index faces commonly associated with single crystals. However, the surface to volume ratio of the supported particles is many orders of magnitude higher than an equivalent amount of bulk metal. In fact, it is not uncommon to use catalysts with 1 nm sized metal particles where nearly every atom can be exposed to the reaction environment.

Estimation of the number of exposed metal atoms is rather straightforward in the case of a single crystal of metal since the geometric surface area can be measured and the number density of surface atoms can be found from the crystal structure.



(a)



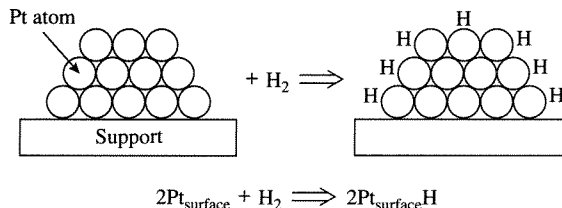
(b)

**Figure 5.1.5 |**

(a) Rhodium metal particles supported on silica carrier. (b) High-resolution electron micrograph shows how small supported Rh crystallites expose low-index faces. (Top photo courtesy of A. K. Datye. Bottom photo from “Modeling of heterogeneous catalysts using simple geometry supports” by A. K. Datye in *Topics in Catalysis*, vol. 13:131, copyright © 2000 by Kluwer Academic, reproduced by permission of the publisher and the author.)

For supported metal catalysts, no simple calculation is possible. A direct measurement of the metal crystallite size or a titration of surface metal atoms is required (see Example 1.3.1). Two common methods to estimate the size of supported crystallites are transmission electron microscopy and X-ray diffraction line broadening analysis. Transmission electron microscopy is excellent for imaging the crystallites, as illustrated in Figure 5.1.5. However, depending on the contrast difference with the support, very small crystallites may not be detected. X-ray diffraction is usually ineffective for estimating the size of very small particles, smaller than about 2 nm. Perhaps the most common method for measuring the number density of exposed metal atoms is selective *chemisorption* of a probe molecule like  $\text{H}_2$ , CO, or  $\text{O}_2$ .

Selective chemisorption uses a probe molecule that does not interact significantly with the support material but forms a strong chemical bond to the surface metal atoms of the supported crystallites. Chemisorption will be discussed in more detail in Section 5.2. Dihydrogen is perhaps the most common probe molecule to measure the fraction of exposed metal atoms. An example of  $\text{H}_2$  chemisorption on Pt is shown below:



The exact stoichiometry of the Pt-H surface complex is still a matter of debate since it depends on the size of the metal particle. For many supported Pt catalysts, an assumption of 1 H atom adsorbing for every 1 Pt surface atom is often a good one. Results from chemisorption can be used to calculate the dispersion of Pt, or the fraction of exposed metal atoms, according to:

$$\text{Fraction exposed} = \text{Dispersion} = \frac{2 \times (\text{H}_2 \text{ molecules chemisorbed})}{\text{Total number of Pt atoms}}$$

If a shape of the metal particle is assumed, its size can be estimated from chemisorption data. For example, a good rule of thumb for spherical particles is to invert the dispersion to get the particle diameter in nanometers:

$$\text{Particle diameter (nm)} = \frac{1}{\text{Dispersion}}$$

Table 5.1.1 compares the average diameter of Pt particles supported on alumina determined by chemisorption of two different probe molecules, X-ray diffraction, and electron microscopy. The excellent agreement among the techniques used to

**Table 5.1.1** | Determination of metal particle size on Pt/Al<sub>2</sub>O<sub>3</sub> catalysts by chemisorption of H<sub>2</sub> and CO, X-ray diffraction, and transmission electron microscopy.

% Pt	Diameter of Pt particles (nm)			
	H <sub>2</sub>	CO	X-ray diffraction	Electron microscopy
0.6 <sup>a</sup>	1.2	1.3	1.3	1.6
2.0 <sup>a</sup>	1.6	1.8	2.2	1.8
3.7 <sup>a</sup>	2.7	2.9	2.7	2.4
3.7 <sup>b</sup>	3.9	—	4.6	5.3

<sup>a</sup>Pretreatment temperature of 500°C.<sup>b</sup>Pretreatment temperature of 800°C.Source: Renouprez et al., *J. Catal.*, **34** (1974) 411.

characterize these model Pt catalysts shows the validity in using chemisorption to estimate particle size.

The reason for measuring the number of exposed metal atoms in a catalyst is that it allows reaction rates to be normalized to the amount of active component. As defined in Chapter 1, the rate expressed per active site is known as the *turnover frequency*,  $r_t$ . Since the turnover frequency is based on the number of active sites, it should not depend on how much metal is loaded into a reactor or how much metal is loaded onto a support. Indeed, the use of turnover frequency has made possible the comparison of rates measured on different catalysts in different laboratories throughout the world.

**VIGNETTE 5.1.2**

Dumesic and co-workers measured the rate of ethylene hydrogenation:



over a variety of Pt catalysts in a flow reactor with a feed of 25 torr of ethylene, 150 torr of dihydrogen, and 585 torr of helium [R. D. Cortright, S. A. Goddard, J. E. Rekoske, and J. A. Dumesic, *J. Catal.*, **127** (1991) 342]. Three of the catalysts consisted of Pt particles supported on Cab-O-Sil silica gel while the fourth was a bulk Pt wire. The fraction of Pt exposed on the supported catalysts, determined by chemisorption of dihydrogen, was 0.7 on the catalyst with 1.2 wt% Pt and unity on the lower loaded Pt catalysts. The number of Pt atoms on the surface of the Pt wire was estimated from the geometric surface area. Figure 5.1.6 shows the temperature dependence of the turnover frequency (TOF) on all of the catalysts at equivalent conditions. Over the entire temperature range, the turnover frequency was found to be independent of the dispersion of the metal. The TOF measured on a bulk Pt wire was virtually the same as that found on 1 nm supported Pt clusters. Reactions that reveal TOFs that are independent of dispersion are called structure insensitive.

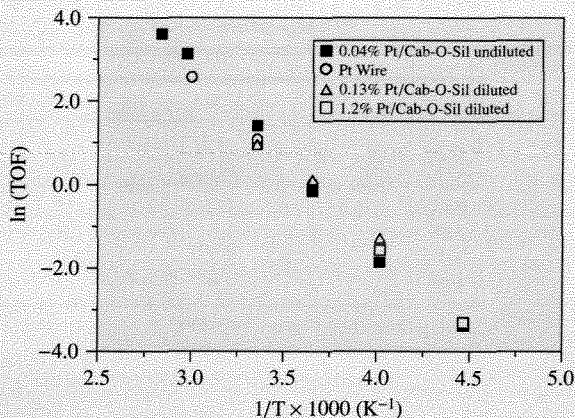


**Figure 5.1.6** | Arrhenius-type plot of the turnover frequency for ethylene hydrogenation on bulk and supported Pt catalysts. (Figure from “Kinetic Study of Ethylene Hydrogenation” by R. D. Cortright, S. A. Goddard, J. E. Rekoske, and J. A. Dumesic, in *Journal of Catalysis*, Volume 127:342, copyright © 1991 by Academic Press, reproduced by permission of the publisher and the authors.)

## 5.2 | Kinetics of Elementary Steps: Adsorption, Desorption, and Surface Reaction

The necessary first step in a heterogeneous catalytic reaction involves activation of a reactant molecule by adsorption onto a catalyst surface. The activation step implies that a fairly strong chemical bond is formed with the catalyst surface. This mode of adsorption is called *chemisorption*, and it is characterized by an enthalpy change typically greater than 80 kJ mol<sup>-1</sup> and sometimes greater than 400 kJ mol<sup>-1</sup>. Since a chemical bond is formed with the catalyst surface, chemisorption is specific in nature, meaning only certain adsorbate-adsorbent combinations are possible. Chemisorption implies that only a single layer, or *monolayer*, of adsorbed molecules is possible since every adsorbed atom or molecule forms a strong bond with the surface. Once the available surface sites are occupied, no additional molecules can be chemisorbed.

Every molecule is capable of weakly interacting with any solid surface through van der Waals forces. The enthalpy change associated with this weak adsorption mode, called *physisorption*, is typically 40 kJ mol<sup>-1</sup> or less, which is far lower than the enthalpy of chemical bond formation. Even though physisorbed molecules are not activated for catalysis, they may serve as precursors to chemisorbed molecules. More than one layer of molecules can physisorb on a surface since only van der Waals interactions are involved. The number of physisorbed molecules that occupy



a monolayer on the surface of any material can be used to calculate its geometric surface area if the cross-sectional area of the adsorbate molecule is known.

**VIGNETTE 5.2.1****BET Method for Evaluation of Surface Area**

In 1919, the Fixed Nitrogen Laboratory was founded in Washington, D.C. to help the United States establish a synthetic ammonia industry. This was done to ensure a reliable supply of nitrate fertilizers and explosives. It was in this laboratory environment that Stephen Brunauer and Paul Emmet worked together to study the adsorption of dinitrogen on promoted iron, the catalyst commonly used in ammonia synthesis reactors today. It became clear to the researchers that some measure of the catalyst surface area was needed to place their studies on a more quantitative basis. After enlisting the help of Edward Teller, then a professor at George Washington University, Brunauer and Emmett were able to describe in very simple terms the phenomenon of multilayer adsorption of weakly adsorbed molecules, or physisorption. Figure 5.2.1 shows a typical physical adsorption isotherm of  $N_2$  on a powdered catalyst surface.

There is no obvious transition in the isotherm that can be attributed to the formation of a complete monolayer of adsorbed  $N_2$ . Brunauer, Emmett, and Teller reasoned that molecules like  $N_2$  do not adsorb on a surface in a layer by layer fashion, but instead begin to form multilayers before completion of a full monolayer. This mode of adsorption is schematically depicted in Figure 5.2.2. The following critical assumptions were made to enable solution of the problem:

1. The layers are densely packed.
2. The heat of adsorption for the first layer is greater than the second (and higher) layers.

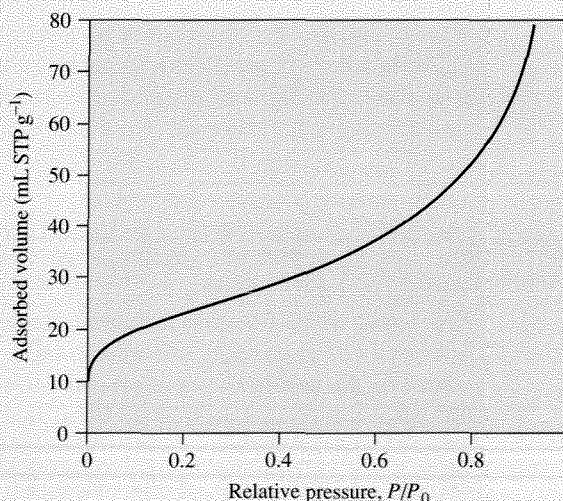


**Figure 5.2.1** | Adsorption of  $N_2$  at 77.3 K on  $\gamma$ -alumina.

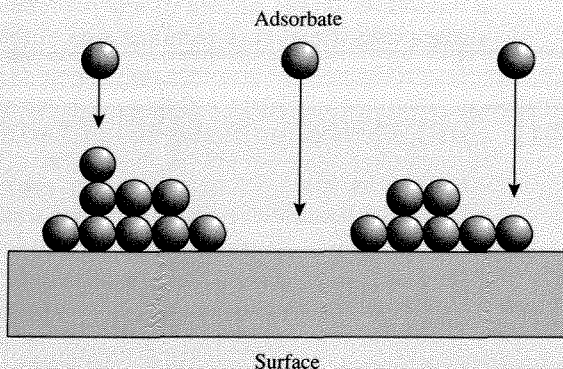


**Figure 5.2.2** | Illustration of multilayer adsorption.

3. The heat of adsorption is constant for all molecules in the first layer.
4. The heat of adsorption for the second (and higher) layers is the same as the heat of liquefaction.

A derivation of the multilayer isotherm is provided in the landmark paper by S. Brunauer, P. H. Emmett, and E. Teller [*J. Am. Chem. Soc.*, **60** (1938) 309] and will not be presented here. The commonly used linearized version of the isotherm developed by Brunauer, Emmett, and Teller bears their initials in the now famous “BET equation”:

$$\frac{P}{V_{\text{ads}}(P_0 - P)} = \frac{1}{cV_m} + \left( \frac{c-1}{cV_m} \right) \frac{P}{P_0} \quad (5.2.1)$$

where  $P$  is the equilibrium pressure of gas with the surface,  $P_0$  is the saturation vapor pressure,  $V_{\text{ads}}$  is the volume of gas (STP) adsorbed by the sample,  $V_m$  is the volume of gas (STP) corresponding to the formation of a monolayer, and  $c$  is a fitted constant. A plot of the left-hand side of Equation (5.2.1) versus  $P/P_0$  yields a straight line having a slope equal to  $(c-1)/(cV_m)$  and an intercept equal to  $1/(cV_m)$ . The volume of gas in a monolayer,  $V_m$ , can then be calculated from fitted values of both the slope and intercept. The best fits to experimental data are obtained by using a restricted pressure range ( $P/P_0$ ) from 0.05 to 0.3. To arrive at a surface area, the number of molecules adsorbed in a monolayer is multiplied by the cross-sectional area of the adsorbing gas. For  $\text{N}_2$ , the molecular cross-sectional area is  $0.162 \text{ nm}^2$ . Even though the BET equation for multilayer adsorption was developed in the late 1930s and involved a few assumptions that are not strictly correct, the universal applicability of the method for determining surface area has allowed its use to continue even today. Indeed, nearly all surface area measurements on powdered catalysts are still analyzed by the BET method. Many commercial instruments perform the so-called one-point BET method. In doing so, the value of  $c$  is assumed to be so large that Equation (5.2.1) reduces to:

$$\frac{P}{V_{\text{ads}}(P_0 - P)} = \left( \frac{1}{V_m} \right) \frac{P}{P_0} \quad (5.2.2)$$

Notice that  $V_m$  can be obtained from one data point ( $V_{ads}$ ,  $P/P_0$ ) by the use of Equation (5.2.2). A problem with this method is that  $c$  may not be large enough to justify simplification of Equation (5.2.1) and is *a priori* usually unknown. Thus, the one-point method is normally useful for analysis of numerous samples of known composition for which  $c$  has been determined.

The potential energy diagram for the chemisorption of hydrogen atoms on nickel is schematically depicted in Figure 5.2.3. As molecular hydrogen approaches the surface, it is trapped in a shallow potential energy well associated with the physisorbed state having an enthalpy of physisorption  $\Delta H_p$ . The deeper well found closer to the surface with enthalpy  $\Delta H_c$  is associated with the hydrogen *atoms* chemisorbed on nickel. There can be an activation barrier to chemisorption,  $E$ , which must be overcome to reach a chemisorbed state from the physisorbed molecule. Since molecular hydrogen (dihydrogen) is dissociated to form chemisorbed hydrogen atoms, this phenomenon is known as *dissociative chemisorption*.

Because rates of heterogeneous catalytic reactions depend on the amounts of chemisorbed molecules, it is necessary to relate the fluid phase concentrations of

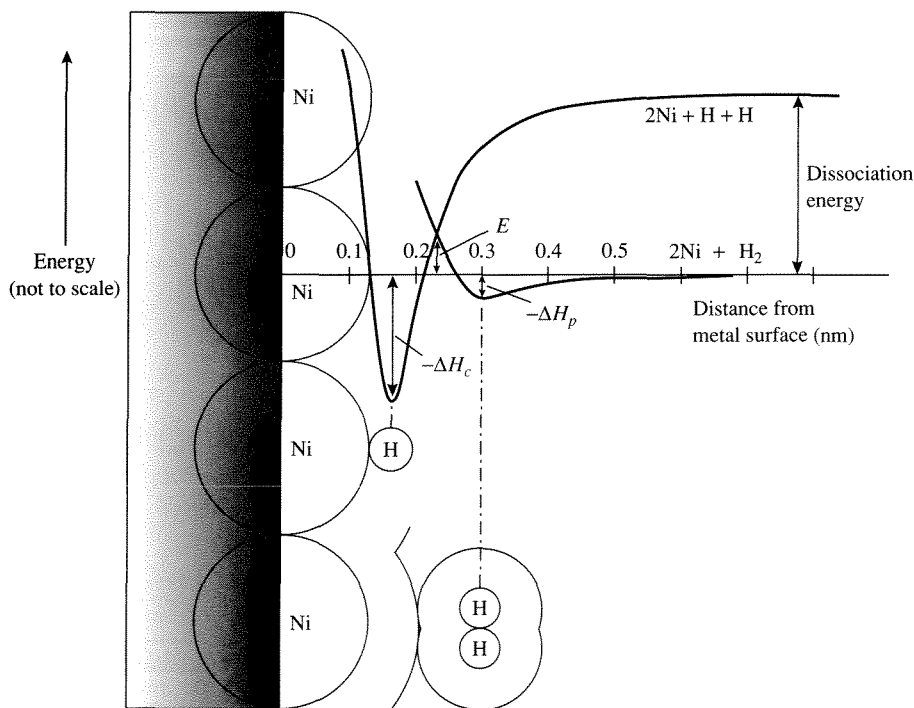
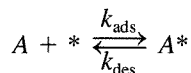


**Figure 5.2.3** |

Potential energy diagram for the chemisorption of hydrogen on nickel.

reactants to their respective coverages on a solid surface. For simplicity, the following discussion assumes that the reactants are present in a single fluid phase (i.e., either liquid or gas), all surface sites have the same energetics for adsorption, and the adsorbed molecules do not interact with each other. The active site for chemisorption on the solid catalyst will be denoted by  $*$ , with a surface concentration  $[*]$ . The adsorption of species  $A$  can then be expressed as:



where  $A^*$  corresponds to  $A$  chemisorbed on a surface site and  $k_{\text{ads}}$  and  $k_{\text{des}}$  refer to the rate constants for adsorption and desorption, respectively. Thus, the net rate of adsorption is given by:

$$r = k_{\text{ads}}[A][*] - k_{\text{des}}[A^*] \quad (5.2.3)$$

Since the net rate of adsorption is zero at equilibrium, the equilibrium relationship is:

$$K_{\text{ads}} = \frac{k_{\text{ads}}}{k_{\text{des}}} = \frac{[A^*]}{[A][*]} \quad (5.2.4)$$

The fractional coverage  $\theta_A$  is defined as the fraction of total surface adsorption sites that are occupied by  $A$ . If  $[*]_0$  represents the number density of all adsorption sites (vacant and occupied) on a catalyst surface, then:

$$[*]_0 = [*] + [A^*] \quad (5.2.5)$$

and

$$\theta_A = \frac{[A^*]}{[*]_0} \quad (5.2.6)$$

Combining Equations (5.2.4–5.2.6) gives expressions for  $[*]$ ,  $[A^*]$ , and  $\theta_A$  in terms of the measurable quantities  $[A]$  and  $K_{\text{ads}}$ :

$$[*] = \frac{[*]_0}{1 + K_{\text{ads}}[A]} \quad (5.2.7)$$

$$[A^*] = \frac{K_{\text{ads}}[A][*]_0}{1 + K_{\text{ads}}[A]} \quad (5.2.8)$$

$$\theta_A = \frac{K_{\text{ads}}[A]}{1 + K_{\text{ads}}[A]} \quad (5.2.9)$$

Equation (5.2.9) is known as the *Langmuir Adsorption Isotherm*, and it is depicted in Figure 5.2.4. At low concentrations of  $A$ , the fractional surface coverage is proportional to  $[A]$ , with a proportionality constant of  $K_{\text{ads}}$ , whereas, at high concentrations of  $A$ , the surface coverage is unity and independent of  $[A]$  (i.e., saturation of the available sites).

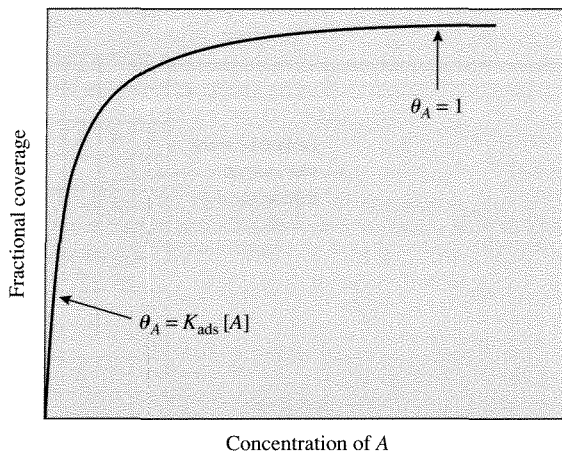


**Figure 5.2.4 |**

Langmuir Adsorption Isotherm: Fractional coverage  $\theta_A$  versus fluid phase concentration of A.

When more than one type of molecule can adsorb on the catalyst surface, the competition for unoccupied sites must be considered. For the adsorption of molecule A in the presence of adsorbing molecule B, the site balance becomes:

$$[*]_0 = [*] + [A*] + [B*]$$

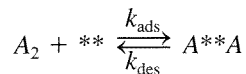
and  $\theta_A$ ,  $\theta_B$  can be expressed as:

$$\theta_A = \frac{K_{\text{ads}A}[A]}{1 + K_{\text{ads}A}[A] + K_{\text{ads}B}[B]} \quad (5.2.10)$$

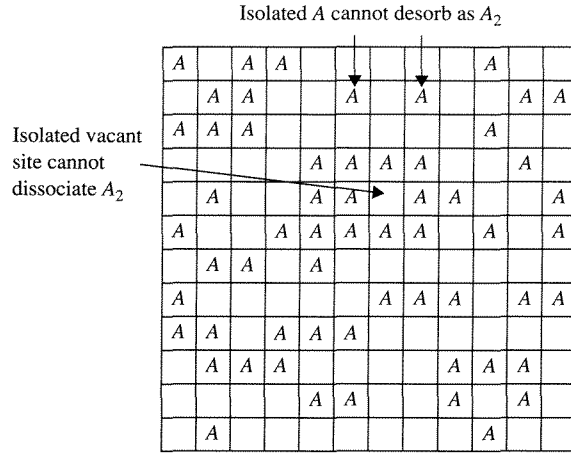
$$\theta_B = \frac{K_{\text{ads}B}[B]}{1 + K_{\text{ads}A}[A] + K_{\text{ads}B}[B]} \quad (5.2.11)$$

where the equilibrium constants are now associated with adsorption/desorption of either A or B.

As mentioned above, some molecules like  $\text{H}_2$  and  $\text{O}_2$  can adsorb dissociatively to occupy two surface sites upon adsorption. The reverse reaction is known as associative desorption. In these cases, the rate of adsorption now depends on the number of *pairs* of available surface sites according to:



where  $**$  refers to a pair of adjacent free sites and  $A^{**}A$  refers to a pair of adjacent occupied sites. M. Boudart and G. Djega-Mariadassou (*Kinetics of Heterogeneous Catalytic Reactions*, Princeton University Press, Princeton, 1984) present expressions for  $[**]$  and  $[A^{**}A]$ , based on the statistics of a partially occupied square

**Figure 5.2.5 |**

Schematic depiction of a square lattice populated by  $A$  atoms. Empty squares represent vacant surface sites.

lattice, shown in Figure 5.2.5. The surface concentrations of adjacent pairs of unoccupied and occupied sites are:

$$[**] = \frac{2[*]^2}{[*]_0} \quad (5.2.12)$$

$$[A**A] = \frac{2[A*]^2}{[*]_0} \quad (5.2.13)$$

Thus, the net rate of dissociative adsorption becomes:

$$r = k_{\text{ads}}[A_2][**] - k_{\text{des}}[A**A]$$

and upon substitution for  $[**]$  and  $[A**A]$  with Equations (5.2.12) and (5.2.13), respectively, gives:

$$r = \frac{2k_{\text{ads}}}{[*]_0}[A_2][*]^2 - \frac{2k_{\text{des}}}{[*]_0}[A*]^2 \quad (5.2.14)$$

The value of two before each rate constant in Equation (5.2.14) is a statistical factor that contains the number of nearest neighbors to an adsorption site on a square lattice and accounts for the fact that indistinguishable neighboring sites should not be double counted. For simplicity, this statistical factor will be lumped into the bimolecular rate constant to yield the following rate expression for dissociative adsorption:

$$r = \frac{k_{\text{ads}}}{[*]_0}[A_2][*]^2 - \frac{k_{\text{des}}}{[*]_0}[A*]^2 \quad (5.2.15)$$

The total number of adsorption sites on the surface now appears explicitly in the rate expression for this elementary adsorption step. Since the site balance is the same as before (Equation 5.2.5), the equilibrium adsorption isotherm can be calculated in the manner described above:

$$K_{\text{ads}} = \frac{k_{\text{ads}}}{k_{\text{des}}} = \frac{[A^*]^2}{[A_2][*]^2} \quad (5.2.16)$$

$$[*] = \frac{[*]_0}{1 + (K_{\text{ads}}[A_2])^{1/2}} \quad (5.2.17)$$

$$[A^*] = \frac{(K_{\text{ads}}[A_2])^{1/2}[*]_0}{1 + (K_{\text{ads}}[A_2])^{1/2}} \quad (5.2.18)$$

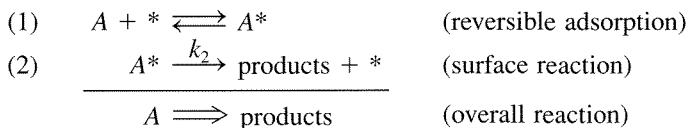
$$\theta_A = \frac{(K_{\text{ads}}[A_2])^{1/2}}{1 + (K_{\text{ads}}[A_2])^{1/2}} \quad (5.2.19)$$

At low concentrations of  $A_2$ , the fractional surface coverage is proportional to  $[A_2]^{1/2}$ , which is quite different than the adsorption isotherm derived above for the case without dissociation. In terms of fractional surface coverage, the net rate of dissociative adsorption is expressed by:

$$r = k_{\text{ads}}[*]_0[A_2](1 - \theta_A)^2 - k_{\text{des}}[*]_0\theta_A^2 \quad (5.2.20)$$

As expected, the rate is proportional to the total number of adsorption sites  $[*]_0$ .

The next step in a catalytic cycle after adsorption of the reactant molecules is a surface reaction, the simplest of which is the unimolecular conversion of an adsorbed species into a product molecule. For example, the following two-step sequence represents the conversion of  $A$  into products through the irreversible surface reaction of  $A$ :



Since the surface reaction is irreversible (one-way), the mechanistic details involved in product formation and desorption are not needed to derive the rate equation. The rate of the overall reaction is:

$$r = k_2[A^*] = k_2[*]_0\theta_A \quad (5.2.21)$$

If the adsorption of  $A$  is nearly equilibrated, the Langmuir adsorption isotherm can be used to find  $\theta_A$ , and the final rate expression simplifies to:

$$r = \frac{k_2 K_{\text{ads}}[*]_0[A]}{1 + K_{\text{ads}}[A]} \quad (5.2.22)$$

**EXAMPLE 5.2.1**

Use the steady-state approximation to derive the rate expression given in Equation (5.2.22).

**■ Answer**

The rate of the reaction is:

$$r = k_2[A^*] \quad (5.2.23)$$

To solve the problem,  $[A^*]$  and  $[*]$  must be evaluated by utilizing the site balance:

$$[*]_0 = [A^*] + [*] \quad (5.2.24)$$

and the steady-state approximation:

$$\frac{d[A^*]}{dt} = 0 = k_{\text{ads}}[A][*] - k_{\text{des}}[A^*] - k_2[A^*] \quad (5.2.25)$$

Solving Equations (5.2.24) and (5.2.25) simultaneously yields the following expression for the concentration of reactive intermediate:

$$[A^*] = \frac{\left(\frac{k_{\text{ads}}}{k_{\text{des}}}\right)[A][*]_0}{1 + \left(\frac{k_{\text{ads}}}{k_{\text{des}}}\right)[A] + \frac{k_2}{k_{\text{des}}}} \quad (5.2.26)$$

The ratio  $k_{\text{ads}}/k_{\text{des}}$  is simply the adsorption equilibrium constant  $K_{\text{ads}}$ . Thus, the rate expression in Equation (5.2.23) can be rewritten as:

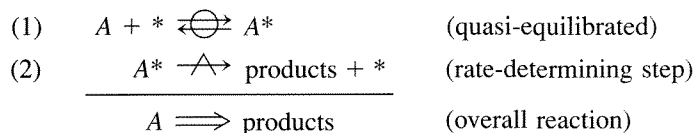
$$r = \frac{k_2 K_{\text{ads}}[A][*]_0}{1 + K_{\text{ads}}[A] + \frac{k_2}{k_{\text{des}}}} \quad (5.2.27)$$

by using Equation (5.2.26) together with  $K_{\text{ads}}$ , and is the same as Equation (5.2.22) except for the last term in the denominator. The ratio  $k_2/k_{\text{des}}$  represents the likelihood of  $A^*$  reacting to form product compared to simply desorbing from the surface. Equation (5.2.22) is based on the assumption that adsorption of  $A$  is nearly equilibrated, which means  $k_{\text{des}}$  is much greater than  $k_2$ . Thus, for this case,  $k_2/k_{\text{des}}$  can be ignored in the denominator of Equation (5.2.27).

The previous discussion involved a two-step sequence for which the adsorption of reactant is nearly equilibrated (quasi-equilibrated). The free energy change associated with the quasi-equilibrated adsorption step is negligible compared to



that of the surface reaction step. The surface reaction is thus called the *rate-determining step* (RDS) since nearly all of the free energy change for the overall reaction is associated with that step. In general, if a rate determining step exists, all other steps in the catalytic sequence are assumed to be quasi-equilibrated. The two-step sequence discussed previously is written in the notation outlined in Chapter 1 as:



The intrinsic rate at which a catalytic cycle turns over on an active site is called the *turnover frequency*,  $r_t$ , of a catalytic reaction and is defined as in Chapter 1 [Equation (1.3.9)] as:

$$r_t = \frac{1}{\bar{S}} \frac{dn}{dt} \quad (5.2.28)$$

where  $\bar{S}$  is the number of active sites in the experiment. As mentioned earlier, quantifying the number of active sites on a surface is problematic. With metals and some metal oxides, often the best one can do is to count the total number of exposed surface atoms per unit surface area as an approximation of  $[*]_0$ . Thus, the turnover frequency for the reaction rate expressed by Equation (5.2.22) is calculated by simply dividing the rate by  $[*]_0$ :

$$r_t = \frac{r}{[*]_0} = \frac{k_2 K_{\text{ads}} [A]}{1 + K_{\text{ads}} [A]} \quad (5.2.29)$$

Surface atoms on real catalysts reside in a variety of coordination environments depending on the exposed crystal plane (see Figure 5.1.3) and may exhibit different catalytic activities in a given reaction. Thus, a turnover frequency based on  $[*]_0$  will be an average value of the catalytic activity. In fact, the calculated turnover frequency is a lower bound to the true activity because only a fraction of the total number of surface atoms may contribute to the reaction rate. Nevertheless, the concept of a turnover frequency on a uniform surface has proven to be very useful in relating reaction rates determined on metal single crystals, metal foils, and supported metal particles.

### VIGNETTE 5.2.2

Ladas et al. measured the rate of CO oxidation by  $O_2$  on a variety of  $Al_2O_3$ -supported Pd catalysts at 445 K, CO pressure equal to  $1.2 \times 10^{-4}$  Pa, and  $P_{O_2}/P_{CO}$  equal to 1.1 [S. Ladas, H. Poppa, and M. Boudart, *Surf. Sci.*, **102** (1981) 151]. The alumina was a flat single crystal onto which Pd particles were deposited by a metal evaporation method. The resulting Pd particle size was measured directly by transmission electron microscopy.

**Table 5.2.1** | Turnover rates<sup>a</sup> of ammonia synthesis at 678 K, stoichiometric feed, 1 atm.

Catalyst	Particle size (nm)	$r_t (\times 10^3 \text{ s}^{-1})$
1% Fe/MgO	1.5	1.0
5% Fe/MgO	4.0	9.0
40% Fe/MgO	30.0	35.0

<sup>a</sup>Rates measured at constant conversion (15% of equilibrium).

Source: J. A. Dumesic, H. Topsøe, and M. Boudart, *J. Catal.*, **37** (1975) 513.

Ladas et al. found that the turnover frequency, based on exposed Pd atoms determined by CO chemisorption, was  $0.012 \text{ s}^{-1}$  and independent of Pd particle size over the range of 1.5 to 8 nm. Thus, CO oxidation is classified as a *structure insensitive* reaction.

A very different result is found when ammonia synthesis is catalyzed by supported iron particles. The results in Table 5.2.1 indicate that the turnover frequency for ammonia synthesis varies by more than one order of magnitude as the Fe particle size changes from 1.5 to 30 nm. Ammonia synthesis on iron is therefore called *structure sensitive* since the turnover frequency varies significantly with particle size. Because the reaction rate does not scale proportionally with the number of surface metal atoms, the active site consists of a group, or *ensemble*, of surface atoms arranged in a particular configuration. Selective chemisorption of  $\text{N}_2$  (instead of  $\text{H}_2$  or CO) can be used to count these specific ensembles on Fe particles. Indeed, the dependence of the turnover frequency on Fe particle size vanishes when the active site density is based on  $\text{N}_2$  chemisorption [H. Topsøe, N. Topsøe, H. Bohlbro, and J. A. Dumesic, *Proc. 7th Int. Cong. Catalysis*, T. Seiyama and K. Tanabe, Eds. (Kodansha: Tokyo) 1981, p. 247].

The presence of poisons or alloy additions can dramatically alter the observed rate of a structure sensitive reaction whereas the rates of structure insensitive reactions are much less affected. Sinfelt et al. studied ethane hydrogenolysis to form methane (a structure sensitive reaction) and cyclohexane dehydrogenation to benzene (a structure insensitive reaction) over a series of Ni-Cu alloys [J. H. Sinfelt, J. L. Carter, and D. J. C. Yates, *J. Catal.*, **24** (1972) 283]. Nickel is the active component for both reactions. The data provided in Figure 5.2.6 show that the rate of cyclohexane dehydrogenation was affected very little by alloying Cu into Ni over a wide range of alloy composition. In contrast, the rate of ethane hydrogenolysis decreased by many orders of magnitude with the small addition of copper.

These results can be easily rationalized if ethane hydrogenolysis requires an ensemble of multiple Ni surface atoms to form an active site. The concentration of active ensembles will decline sharply with composition as the active Ni atoms are diluted with inactive Cu atoms in the surface. Additional information on how bimetallic catalysts affect chemical reactions can be found in the excellent monograph by Sinfelt (J. H. Sinfelt, *Bimetallic Catalysts: Discoveries, Concepts, and Applications*, Wiley, New York, 1983).

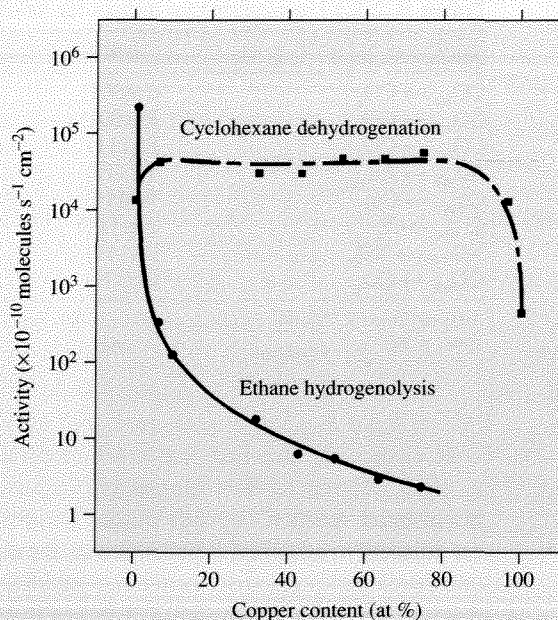


**Figure 5.2.6** | Effect of alloy composition on the rates of ethane hydrogenolysis and cyclohexane dehydrogenation on Ni-Cu catalysts. (Figure from “Catalytic Hydrogenolysis and Dehydrogenation Over Copper-Nickel Alloys” by J. H. Sinfelt, J. L. Carter, and D. J. C. Yates in *Journal of Catalysis*, Volume 24:283, copyright © 1972 by Academic Press, reproduced by permission of the publisher.)

The rate of a structure sensitive reaction catalyzed by a metal single crystal is also a function of the exposed plane. As illustrated in Figure 5.1.3, the low-index planes of common crystal structures have different arrangements of surface atoms. Thus, caution must be exercised when the rates of structure sensitive reactions measured on single crystals are compared to those reported for supported metal particles.

As an extension to concepts discussed earlier, a rate expression for the reaction of  $A$  and  $B$  to form products can be developed by assuming an irreversible, rate-determining, bimolecular surface reaction:

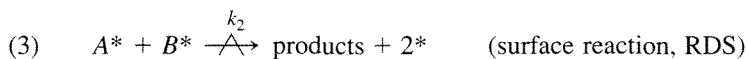


**Table 5.2.2** | Pre-exponential factors for selected unimolecular surface reactions.

Reaction	Surface	Pre-exponential factor ( $\text{s}^{-1}$ )
$\text{CO}_{\text{ads}} \rightarrow \text{CO}_{\text{g}}$	Cu(001)	$10^{14}$
$\text{CO}_{\text{ads}} \rightarrow \text{CO}_{\text{g}}$	Ru(001)	$10^{19.5}$
$\text{CO}_{\text{ads}} \rightarrow \text{CO}_{\text{g}}$	Pt(111)	$10^{14}$
$\text{Au}_{\text{ads}} \rightarrow \text{Au}_{\text{g}}$	W(110)	$10^{11}$
$\text{Cu}_{\text{ads}} \rightarrow \text{Cu}_{\text{g}}$	W(110)	$10^{14.5}$
$\text{Cl}_{\text{ads}} \rightarrow \text{Cl}_{\text{g}}$	Ag(110)	$10^{20}$
$\text{NO}_{\text{ads}} \rightarrow \text{NO}_{\text{g}}$	Pt(111)	$10^{16}$
$\text{CO}_{\text{ads}} \rightarrow \text{CO}_{\text{g}}$	Ni(111)	$10^{15}$

Adapted from R. Masel, *Principles of Adsorption and Reaction on Solid Surfaces*, Wiley, New York, 1996, p. 607.

Before  $A$  and  $B$  can react, they must both adsorb on the catalyst surface. The next event is an elementary step that proceeds through a reaction of adsorbed intermediates and is often referred to as a *Langmuir-Hinshelwood* step. The rate expression for the bimolecular reaction depends on the number density of adsorbed  $A$  molecules that are adjacent to adsorbed  $B$  molecules on the catalyst surface. This case is similar to the one developed previously for the recombinative desorption of diatomic gases [reverse reaction step in Equation (5.2.20)] except that two different atomic species are present on the surface. A simplified rate expression for the bimolecular reaction is:

$$r = k_3 [A^*][B^*]/[*]_0 = k_3 [*]_0 \theta_A \theta_B \quad (5.2.30)$$

where  $\theta_A$  and  $\theta_B$  each can be expressed in the form of the Langmuir isotherm for competitive adsorption of  $A$  and  $B$  that are presented in Equations (5.2.10) and (5.2.11) and  $k_3$  is the rate constant for step 3. Thus, the overall rate of reaction of  $A$  and  $B$  can be expressed as:

$$r = \frac{k_3 K_{\text{ads}A} K_{\text{ads}B} [*]_0 [A][B]}{(1 + K_{\text{ads}A}[A] + K_{\text{ads}B}[B])^2} \quad (5.2.31)$$

Notice that the denominator is squared for a bimolecular surface reaction. In general, the exponent on the denominator is equal to the number of sites participating in a rate-determining surface-catalyzed reaction. Since trimolecular surface events are uncommon, the exponent of the denominator rarely exceeds 2.

It is instructive to compare the values of pre-exponential factors for elementary step rate constants of simple surface reactions to those anticipated by transition state theory. Recall from Chapter 2 that the pre-exponential factor  $\bar{A}$  is on the order of  $kT/h = 10^{13} \text{ s}^{-1}$  when the entropy change to form the transition state is negligible. Some pre-exponential factors for simple unimolecular desorption reactions are presented in Table 5.2.2. For the most part, the entries in the table are within a few orders of magnitude of  $10^{13} \text{ s}^{-1}$ . The very high values of the pre-exponential factor are likely attributed to large increases in the entropy upon formation of the transition state. Bimolecular surface reactions can be treated in the same way. However, one must explicitly account for the total number of surface

**Table 5.2.3** | Pre-exponential factors for  $2\text{H}_{\text{ads}} \rightarrow \text{H}_{2\text{g}}$  on transition metal surfaces.

Surface	Pre-exponential factor <sup>a</sup> ( $\text{s}^{-1}$ )
Pd(111)	$10^{12}$
Ni(100)	$10^{13.5}$
Ru(001)	$10^{14.5}$
Pd(110)	$10^{13.5}$
Mo(110)	$10^{13}$
Pt(111)	$10^{12}$

<sup>a</sup>The values have been normalized by  $[\ast]_0$ .

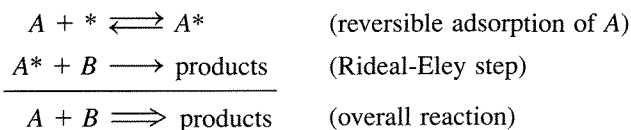
Adapted from R. Masel, *Principles of Adsorption and Reaction on Solid Surfaces*, Wiley, New York, 1996, p. 607.

sites in the rate expression. As discussed above, the rate of associative desorption of  $\text{H}_2$  from a square lattice can be written as:

$$r_{\text{des}} = \frac{2k_{\text{des}}[H^*]^2}{[\ast]_0} \quad (5.2.32)$$

where the pre-exponential factor of the rate constant is now multiplied by  $2/[\ast]_0$  to properly account for the statistics of a reaction occurring on adjacent sites. For desorption of  $\text{H}_2$  at 550 K from a W(100) surface, which is a square lattice with  $[\ast]_0 = 5 \times 10^{14} \text{ cm}^{-2}$ , the pre-exponential factor is anticipated to be  $4.6 \times 10^{-2} \text{ cm}^2 \text{ s}^{-2}$ . The reported experimental value of  $4.2 \times 10^{-2} \text{ cm}^2 \text{ s}^{-1}$  is very close to that predicted by transition state theory (M. Boudart and G. Djega-Mariadassou, *Kinetics of Heterogeneous Catalytic Reactions*, Princeton University Press, Princeton, 1984, p. 71). The measured pre-exponential factors for associative desorption of dihydrogen from other transition metal surfaces (normalized by the surface site density) are summarized in Table 5.2.3. Clearly, the values in Table 5.2.3 are consistent with transition state theory.

A fairly rare elementary reaction between  $A$  and  $B$ , often called a *Rideal-Eley* step, occurs by direct reaction of gaseous  $B$  with adsorbed  $A$  according to the following sequence:

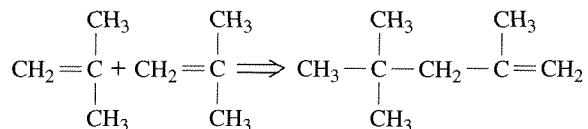


Theoretically, if reactions are able to proceed through either a Rideal-Eley step or a Langmuir-Hinshelwood step, the Langmuir-Hinshelwood route is much more preferred due to the extremely short time scale (picosecond) of a gas-surface collision. The kinetics of a Rideal-Eley step, however, can become important at extreme conditions. For example, the reactions involved during plasma processing of electronic materials

are believed to occur through Rideal-Eley steps. Apparently, the conditions typical of semiconductor growth favor Rideal-Eley elementary steps whereas conditions normally encountered with catalytic reactions favor Langmuir-Hinshelwood steps. This point is thoroughly discussed by R. Masel (*Principles of Adsorption and Reaction on Solid Surfaces*, Wiley, New York, 1996, pp. 444–448).

### EXAMPLE 5.2.2

A reaction that is catalyzed by a Bronsted acid site, or  $H^+$ , can often be accelerated by addition of a solid acid. Materials like ion-exchange resins, zeolites, and mixed metal oxides function as solid analogues of corrosive liquid acids (e.g.,  $H_2SO_4$  and  $HF$ ) and can be used as acidic catalysts. For example, isobutylene (IB) reacts with itself to form dimers on cross-linked poly(styrene-sulfonic acid), a strongly acidic solid polymer catalyst:



The kinetics of IB dimerization are presented in Figure 5.2.7 for two different initial concentrations of IB in hexane solvent. The reaction appears to be first order at high

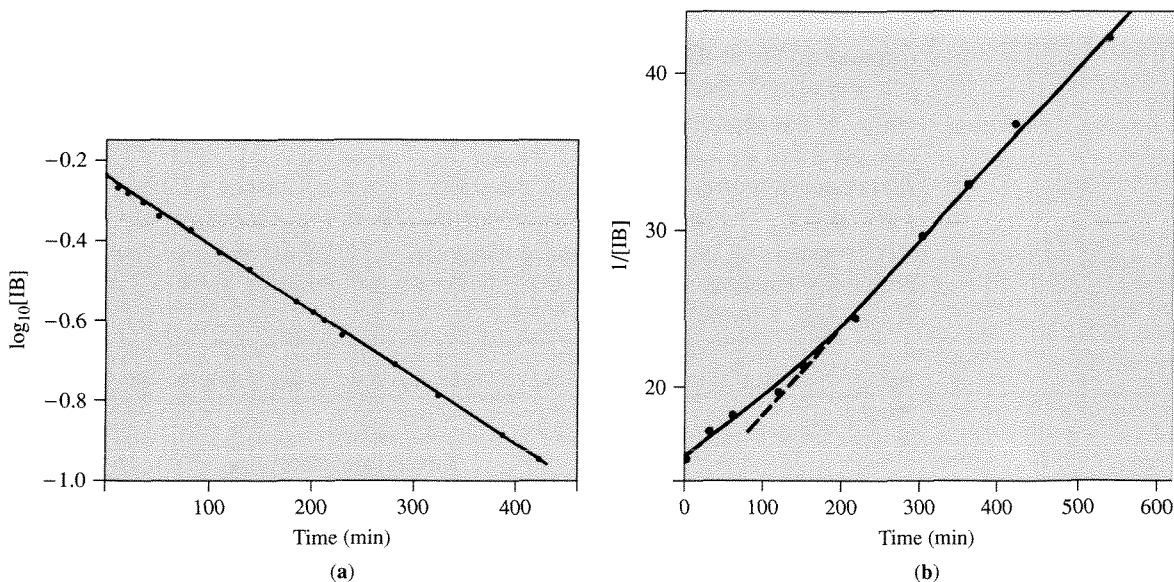


**Figure 5.2.7** | Kinetics of liquid phase oligomerization of isobutylene catalyzed by poly(styrene-sulfonic acid) at 20°C in hexane solvent. (a) Corresponds to high initial concentration of isobutylene. (b) Corresponds to low initial concentration of isobutylene. [Figures from W. O. Haag, *Chem. Eng. Prog. Symp. Ser.*, **63** (1967) 140. Reproduced with permission of the American Institute of Chemical Engineers. Copyright © 1967 AIChE. All rights reserved.]

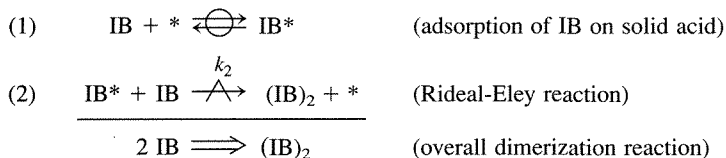
concentrations of IB since a logarithmic plot of [IB] with respect to reaction time is linear. At low concentrations, however, the reaction shifts to second order since a plot of  $1/[IB]$  as a function of time becomes linear. A rate expression consistent with these results is:

$$r = \frac{\bar{\alpha}_1 [IB]^2}{1 + \bar{\alpha}_2 [IB]} \quad (5.2.33)$$

where  $\bar{\alpha}_1$  and  $\bar{\alpha}_2$  are constants. Show how a rate expression of this form can be derived for this reaction.

### ■ Answer

The following two-step catalytic cycle for dimerization of IB is proposed.



In this case, \* represents a surface acid site and IB\* designates an adsorbed t-butyl cation. Notice that step 2 involves the combination of an adsorbed reactant with one present in the liquid phase. The rate equation takes the form:

$$r = k_2 [IB^*] [IB] \quad (5.2.34)$$

The concentration of adsorbed IB is found by combining the equilibrium relationship for step 1 and the overall site balance to give:

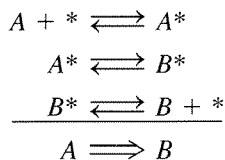
$$[IB^*] = \frac{K_{\text{ads}} [^*]_0 [IB]}{1 + K_{\text{ads}} [IB]} \quad (5.2.35)$$

where  $[^*]_0$  represents the total number of acid sites on the catalyst surface, and  $K_{\text{ads}}$  is the adsorption equilibrium constant of IB. Substitution of Equation (5.2.35) into (5.2.34) yields a final form of the rate expression:

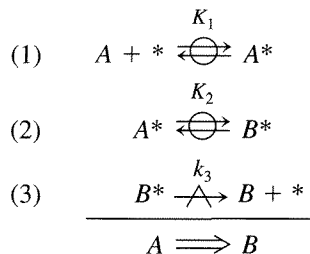
$$r = \frac{k_2 K_{\text{ads}} [^*]_0 [IB]^2}{1 + K_{\text{ads}} [IB]} \quad (5.2.36)$$

that has the same functional form as Equation (5.2.33) with  $\bar{\alpha}_1 = k_2 K_{\text{ads}} [^*]_0$  and  $\bar{\alpha}_2 = K_{\text{ads}}$  and is consistent with the experimental data shown in Figure 5.2.7.

The rate of product desorption can also influence the kinetics of a surface-catalyzed reaction. Consider the following simple catalytic cycle:



If desorption of  $B$  from the surface is rate-determining, then all elementary steps prior to desorption are assumed to be quasi-equilibrated:



The overall rate in the forward direction only is given by:

$$r = r_3 = k_3[B^*] \quad (5.2.37)$$

The rate expression is simplified by eliminating surface concentrations of species through the use of appropriate equilibrium relationships. According to step (2):

$$[B^*] = K_2[A^*] \quad (5.2.38)$$

and thus:

$$r = k_3 K_2[A^*] \quad (5.2.39)$$

To find  $[A^*]$ , the equilibrium adsorption relationship is used:

$$K_1 = \frac{[A^*]}{[A][*]} \quad [A^*] = K_1[A][*] \quad (5.2.40)$$

which gives:

$$r = k_3 K_2 K_1 [A][*] \quad (5.2.41)$$

The concentration of vacant sites on the surface is derived from the total site balance:

$$\begin{aligned}
 [*]_0 &= [*] + [A^*] + [B^*] \\
 [*]_0 &= [*] + [A^*] + K_2[A^*] \\
 [*]_0 &= [*] + K_1[A][*] + K_2 K_1[A][*] \\
 [*] &= \frac{[*]_0}{1 + (K_1 + K_2 K_1)[A]}
 \end{aligned} \quad (5.2.42)$$

Substitution of Equation (5.2.42) into Equation (5.2.41) gives the final rate expression as:

$$r = \frac{k_3 K_2 K_1 [A][*]_0}{1 + (K_1 + K_2 K_1)[A]} \quad (5.2.43)$$

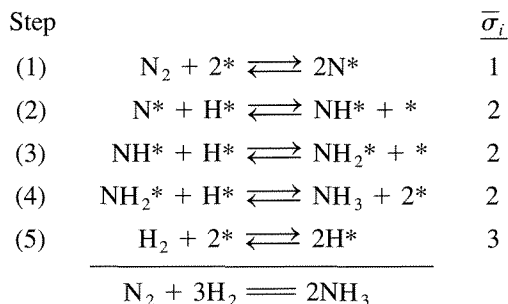
Notice the rate expression for this case does not depend on the product concentration.



### 5.3 | Kinetics of Overall Reactions

Consider the entire sequence of elementary steps comprising a surface-catalyzed reaction: adsorption of reactant(s), surface reaction(s), and finally desorption of product(s). If the surface is considered uniform (i.e., all surface sites are identical kinetically and thermodynamically), and there are negligible interactions between adsorbed species, then derivation of overall reaction rate equations is rather straightforward.

For example, the reaction of dinitrogen and dihydrogen to form ammonia is postulated to proceed on some catalysts according to the following sequence of elementary steps:

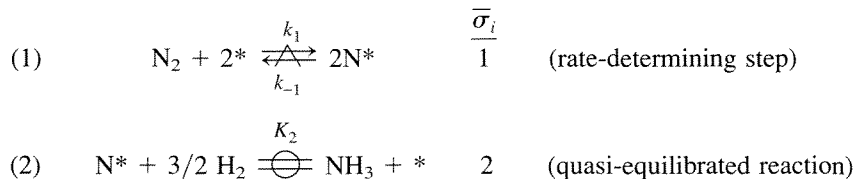


where  $\bar{\sigma}_i$  is the stoichiometric number of elementary step  $i$  and defines the number of times an elementary step must occur in order to complete one catalytic cycle according to the overall reaction. In the sequence shown above,  $\bar{\sigma}_2 = 2$  means that step 2 must occur twice for every time that a dinitrogen molecule dissociately adsorbs in step 1. The net rate of an overall reaction can now be written in terms of the rate of any one of the elementary steps, weighted by the appropriate stoichiometric number:

$$r = \frac{r_i - r_{-i}}{\bar{\sigma}_i} \quad (5.3.1)$$

The final form of a reaction rate equation from Equation (5.3.1) is derived by repeated application of the steady-state approximation to eliminate the concentrations of reactive intermediates.

In many cases, however, the sequence of kinetically relevant elementary steps can be reduced to two steps (M. Boudart and G. Djega-Mariadassou, *Kinetics of Heterogeneous Catalytic Reactions*, Princeton University Press, Princeton, 1984, p. 90). For example, the sequence given above for ammonia synthesis can be greatly simplified by assuming step 1 is rate-determining and all other steps are nearly equilibrated. The two relevant steps are now:



It must be emphasized that step 2 is not an elementary step, but a sum of all of the quasi-equilibrated steps that must occur after dinitrogen adsorption. According to this abbreviated sequence, the only species on the surface of the catalyst of any kinetic relevance is  $N^*$ . Even though the other species ( $H^*$ ,  $NH^*$ , etc.) may also be present, according to the assumptions in this example only  $N^*$  contributes to the site balance:

$$[*]_0 = [N^*] + [*] \quad (5.3.2)$$

In a case such as this one where only one species is present in appreciable concentration on the surface, that species is often referred to as the *most abundant reaction intermediate*, or *mari*. The overall rate of reaction can be expressed as the rate of dissociative adsorption of  $N_2$ :

$$r = r_1 - r_{-1} = \frac{k_1[N_2][*]^2}{[*]_0} - \frac{k_{-1}[N^*]^2}{[*]_0} \quad (5.3.3)$$

where  $[*]$  and  $[N^*]$  are determined by the equilibrium relationship for step 2:

$$K_2 = \frac{[N^*][H_2]^{3/2}}{[NH_3][*]} \quad (5.3.4)$$

and the site balance. The constant  $K_2$  is written in such a way that it is large when  $[N^*]$  is also large. Solving Equations (5.3.2) and (5.3.4) for  $[*]$  and  $[N^*]$ , respectively, yields:

$$[*] = \frac{[*]_0}{1 + K_2 \left( \frac{[NH_3]}{[H_2]^{3/2}} \right)} \quad (5.3.5)$$

$$[N^*] = \frac{K_2 \left( \frac{[NH_3]}{[H_2]^{3/2}} \right) [*]_0}{1 + K_2 \left( \frac{[NH_3]}{[H_2]^{3/2}} \right)} \quad (5.3.6)$$

Substitution of Equations (5.3.5) and (5.3.6) into (5.3.3) gives the rate equation for the reaction as:

$$r = \frac{k_1[*]_0[N_2] - k_{-1}K_2^2[*]_0^2 \left( \frac{[NH_3]^2}{[H_2]^3} \right)}{\left[ 1 + K_2 \left( \frac{[NH_3]}{[H_2]^{3/2}} \right) \right]^2} \quad (5.3.7)$$

At very low conversion (far from equilibrium), the reverse reaction can be neglected thus simplifying the rate expression to:

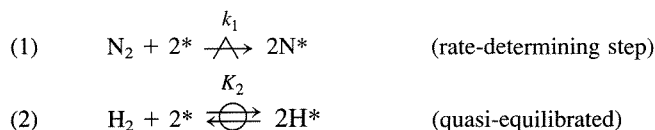
$$r = \frac{k_1[*]_0[N_2]}{\left[ 1 + K_2 \left( \frac{[NH_3]}{[H_2]^{3/2}} \right) \right]^2} \quad (5.3.8)$$

**EXAMPLE 5.3.1**

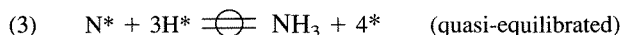
Ruthenium has been investigated by many laboratories as a possible catalyst for ammonia synthesis. Recently, Becue et al. [T. Becue, R. J. Davis, and J. M. Garces, *J. Catal.*, **179** (1998) 129] reported that the forward rate (far from equilibrium) of ammonia synthesis at 20 bar total pressure and 623 K over base-promoted ruthenium metal is first order in dinitrogen and inverse first order in dihydrogen. The rate is very weakly inhibited by ammonia. Propose a plausible sequence of steps for the catalytic reaction and derive a rate equation consistent with experimental observation.

**■ Answer**

In the derivation of Equation (5.3.8), dissociative adsorption of dinitrogen was assumed to be the rate-determining step and this assumption resulted in a first-order dependence of the rate on dinitrogen. The same step is assumed to be rate-determining here. However, the rate expression in Equation (5.3.8) has an overall positive order in dihydrogen. Therefore, some of the assumptions used in the derivation of Equation (5.3.8) will have to be modified. The observed negative order in dihydrogen for ammonia synthesis on ruthenium suggests that H atoms occupy a significant fraction of the surface. If  $H^*$  is assumed to be the most abundant reaction intermediate on the surface, an elementary step that accounts for adsorption of dihydrogen must be included explicitly. Consider the following steps:



that are followed by many surface reactions to give an overall equilibrated reaction represented by:



As before, the forward rate of the reaction (far from equilibrium) can be expressed in terms of the rate-determining step:

$$r = r_1 = \frac{k_1[N_2][^*]^2}{[^*]_0} \quad (5.3.9)$$

To eliminate  $[^*]$  from Equation (5.3.9), use the equilibrium relationship for step 2 combined with the site balance. Hence, the following equations:

$$K_2 = \frac{[H^*]^2}{[^*]^2[H_2]} \quad (5.3.10)$$

$$[^*]_0 = [H^*] + [^*] \quad (5.3.11)$$

are solved simultaneously to give:

$$[^*] = \frac{[^*]_0}{1 + K_2^{1/2}[H_2]^{1/2}} \quad (5.3.12)$$

Substitution of Equation (5.3.12) into Equation (5.3.9) provides the final rate equation:

$$r = \frac{k_1[^*]_0[N_2]}{(1 + K_2^{1/2}[H_2]^{1/2})^2} \quad (5.3.13)$$

If the surface is nearly covered with adsorbed H atoms, then:

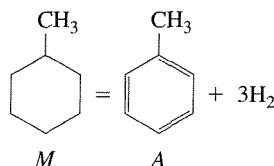
$$K_2^{1/2}[H_2]^{1/2} \gg 1 \quad (5.3.14)$$

and the rate equation simplifies to:

$$r = \left( \frac{k_1[^*]_0}{K_2} \right) \frac{[N_2]}{[H_2]} \quad (5.3.15)$$

This expression is consistent with the experimental observations. For this example, the reaction equilibrium represented by step 3 is never used to solve the problem since the most abundant reaction intermediate is assumed to be H\* (accounted for in the equilibrated step 2.) Thus, a complex set of elementary steps is reduced to two kinetically significant reactions.

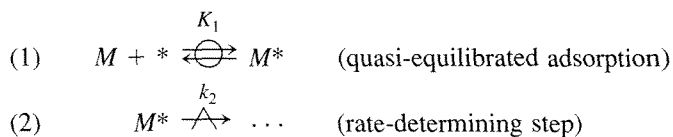
The concept that a multistep reaction can often be reduced to two kinetically significant steps is illustrated again by considering the dehydrogenation of methylcyclohexane to toluene on a Pt/Al<sub>2</sub>O<sub>3</sub> reforming catalyst [J. H. Sinfelt, H. Hurwitz and R. A. Shulman, *J. Phys. Chem.*, **64** (1960)1559]:



The observed rate expression for the reaction operated far from equilibrium can be written in the form:

$$r = \frac{\bar{\alpha}_1[M]}{1 + \bar{\alpha}_2[M]} \quad (5.3.16)$$

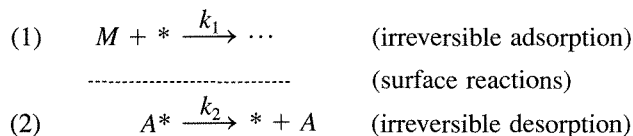
The reaction occurs through a complex sequence of elementary steps that includes adsorption of *M*, surface reactions of *M*\*, and partially dehydrogenated *M*\*, and finally desorption of both H<sub>2</sub> and toluene. It may be possible, however, to simplify this multistep sequence. Consider the following two step sequence that involves *M*\* as the *mari*:



The site balance and the Langmuir adsorption isotherm can be used to derive the forward rate expression:

$$r = r_2 = k_2[M^*] = \frac{k_2 K_1 [^*]_0 [M]}{1 + K_1 [M]} \quad (5.3.17)$$

that has the same form as the observed rate expression, Equation (5.3.16). A word of caution is warranted at this point. *The fact that a proposed sequence is consistent with observed kinetics does not prove that a reaction actually occurs by that pathway.* Indeed, an alternative sequence of steps can be proposed for the above reaction:



The application of the quasi-steady-state approximation and the site balance (assuming  $A^*$  is the *mari*) gives the following expression for the reaction rate:

$$r = r_2 = k_2[A^*] = \frac{k_2(k_1/k_2)[^*]_0[M]}{1 + (k_1/k_2)[M]} = \frac{k_1[^*]_0[M]}{1 + (k_1/k_2)[M]} \quad (5.3.18)$$

The functional form of the rate equation in Equation (5.3.18) is identical to that of Equation (5.3.17), illustrating that two completely different sets of assumptions can give rate equations consistent with experimental observation. Clearly, more information is needed to discriminate between the two cases. Additional experiments have shown that benzene added to the methylcyclohexane feed inhibits the rate only slightly. In the first case, benzene is expected to compete with methylcyclohexane for available surface sites since  $M$  is equilibrated with the surface. In the second case,  $M$  is not equilibrated with the surface and the irreversibility of toluene desorption implies that the surface coverage of toluene is far above its equilibrium value. Benzene added to the feed will not effectively displace toluene from the surface since benzene will cover the surface only to the extent of its equilibrium amount. The additional information provided by the inclusion of benzene in the feed suggests that the second case is the preferred path.

It is possible to generalize the treatment of single-path reactions when a most abundant reaction intermediate (*mari*) can be assumed. According to M. Boudart and G. Djega-Mariadassou (*Kinetics of Heterogeneous Catalytic Reactions*, Princeton University Press, Princeton, 1984, p. 104) three rules can be formulated:

1. If in a sequence, the rate-determining step produces or destroys the *mari*, the sequence can be reduced to two steps, an adsorption equilibrium and the rate-determining step, with all other steps having no kinetic significance.
2. If all steps are practically irreversible and there exists a *mari*, only two steps need to be taken into account: the adsorption step and the reaction (or desorption) step

of the *mari*. All other steps have no kinetic significance. In fact, they may be reversible, in part or in whole.

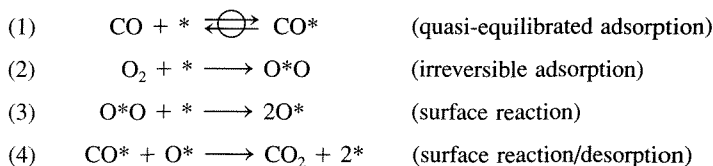
3. All equilibrated steps following a rate-determining step that produces the *mari* may be summed up in an overall equilibrium reaction. Similarly, all equilibrated steps that precede a rate-determining step that consumes the *mari* may be represented by a single overall equilibrium reaction.

The derivation of a rate equation from two-step sequences can also be generalized. First, if the rate-determining step consumes the *mari*, the concentration of the latter is obtained from the equilibrium relationship that is available. Second, if the steps of the two-step sequence are practically irreversible, the steady-state approximation leads to the solution.

These simplifying assumptions must be adapted to some extent to explain the nature of some reactions on catalyst surfaces. The case of ammonia synthesis on supported ruthenium described in Example 5.3.1 presents a situation that is similar to rule 1, except the rate-determining step does not involve the *mari*. Nevertheless, the solution of the problem was possible. Example 5.3.2 involves a similar scenario. If a *mari* cannot be assumed, then a rate expression can be derived through repeated use of the steady-state approximation to eliminate the concentrations of reactive intermediates.

### EXAMPLE 5.3.2

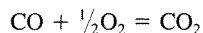
The oxidation of carbon monoxide on palladium single crystals at low pressures (between  $10^{-8}$  and  $10^{-6}$  torr) and temperatures ranging from about 450 to 550 K follows a rate law that is first order in  $O_2$  and inverse first order in CO. An appropriate sequence of elementary steps is:



If  $CO^*$  is assumed to be the *mari*, derive the rate expression.

#### ■ Answer

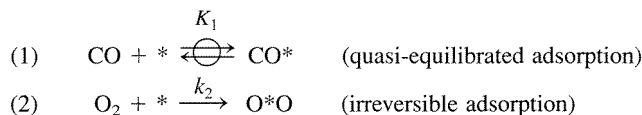
The rate of reaction is the rate of any single step in the sequence weighted by its appropriate stoichiometric number. Thus, for the reaction:



the rate can be written:

$$r = (r_1 - r_{-1}) = 2r_2 = 2r_3 = r_4 \quad (5.3.19)$$

The simplest solution involves the two-step sequence:



where:

$$r = 2r_2 = 2k_2[\text{O}_2][*] \quad (5.3.20)$$

Application of the site balance, assuming  $\text{CO}^*$  is the *major* gives:

$$[*]_0 = [*] + [\text{CO}^*] \quad (5.3.21)$$

and the Langmuir isotherm for adsorption of CO can be written as:

$$K_1 = \frac{[\text{CO}^*]}{[\text{CO}][*]} \quad (5.3.22)$$

Substitution of Equations (5.3.21) and (5.3.22) into Equation (5.3.20) yields:

$$r = \frac{2k_2[*]_0[\text{O}_2]}{1 + K_1[\text{CO}]} \quad (5.3.23)$$

At high values of surface coverage,  $K_1[\text{CO}] \gg 1$ , the rate equation simplifies to:

$$r = \frac{2k_2[*]_0[\text{O}_2]}{K_1[\text{CO}]} \quad (5.3.24)$$

which is consistent with the observed rate law.

The rate constant for the reaction is composed of two terms,  $2k_2$  and  $K_1^{-1}$ . Thus, the apparent activation energy contains contributions from the rate constant for  $\text{O}_2$  adsorption and the equilibrium constant for CO adsorption according to:

$$E_{\text{app}} = E_2 - \Delta H_{\text{adsCO}} \quad (5.3.25)$$

Since adsorption of  $\text{O}_2$  is essentially nonactivated, the apparent activation energy for CO oxidation is simply the negative of the enthalpy of CO adsorption on Pd. This result has been experimentally observed [M. Boudart, *J. Mol. Catal. A: Chem.*, **120** (1997) 271].

Example 5.3.2 demonstrates how the heat of adsorption of reactant molecules can profoundly affect the kinetics of a surface catalyzed chemical reaction. The experimentally determined, apparent rate constant ( $2k_2/K_1$ ) shows typical Arrhenius-type behavior since it increases exponentially with temperature. The apparent activation energy of the reaction is simply  $E_{\text{app}} = E_2 - \Delta H_{\text{adsCO}} \cong -\Delta H_{\text{adsCO}}$  (see Example 5.3.2), which is a positive number. A situation can also arise in which a *negative* overall activation energy is observed, that is, the observed reaction rate

decreases with increasing temperature. This seemingly odd phenomenon can be understood in terms of the multistep mechanism of surface catalyzed reactions. Consider the rate of conversion of  $A$  occurring through a rate-determining surface reaction as described earlier:

$$r = \frac{k_2 K_{\text{ads}} [^*]_0 [A]}{1 + K_{\text{ads}} [A]} \quad (5.3.26)$$

Experimental conditions can arise so that  $1 \gg K_{\text{ads}} [A]$ , and the reaction rate expression reduces to:

$$r = k_2 K_{\text{ads}} [^*]_0 [A] \quad (5.3.27)$$

with an apparent rate constant  $k_2 K_{\text{ads}}$ . The apparent activation energy is now:

$$E_{\text{app}} = E_2 + \Delta H_{\text{ads}} \quad (5.3.28)$$

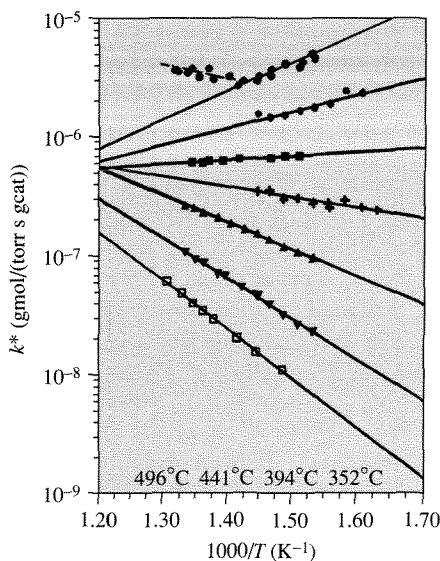


**Figure 5.3.1 |**

Temperature dependence of the cracking of n-alkanes. [Reprinted from J. Wei, "Adsorption and Cracking of N-Alkanes over ZSM-5: Negative Activation Energy of Reaction," *Chem. Eng. Sci.*, **51** (1996) 2995, with permission from Elsevier Science.]  
 Open square— $C_8$ , inverted triangle— $C_{10}$ , triangle— $C_{12}$ , plus— $C_{14}$ , filled square— $C_{16}$ , diamond— $C_{18}$ , circle— $C_{20}$ .



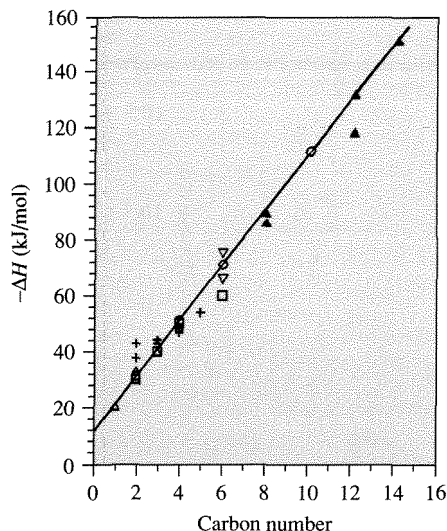


**Figure 5.3.2 |**

Heats of adsorption of n-alkanes on ZSM-5.

[Reprinted from J. Wei, "Adsorption and Cracking of N-Alkanes over ZSM-5: Negative Activation Energy of Reaction," *Chem. Eng. Sci.*, **51** (1996) 2995, with permission from Elsevier Science.]

Since the enthalpy of adsorption is almost always negative, the apparent activation energy can be either positive or negative, depending on the magnitudes of  $E_2$  and  $\Delta H_{\text{ads}}$ .

The cracking of n-alkanes over H-ZSM-5, an acidic zeolite, provides a clear illustration of how the apparent activation energy can be profoundly affected by the enthalpy of adsorption. An Arrhenius plot of the pseudo-first-order rate constant,  $k^* = k_2 K_{\text{ads}}$ , for n-alkanes having between 8 and 20 carbon atoms is shown in Figure 5.3.1. The reaction of smaller alkanes ( $\text{C}_8$ – $\text{C}_{14}$ ) has a positive apparent activation energy that declines with chain length, whereas the reaction of larger alkanes ( $\text{C}_{18}$ ,  $\text{C}_{20}$ ) has a negative apparent activation energy that becomes more negative with chain length. Interestingly, the reaction of  $\text{C}_{16}$  is almost invariant to temperature. The linear relationship in Figure 5.3.2 demonstrates that the adsorption enthalpy is proportional to the number of carbons in the alkanes. Thus, if the activation energy of the surface reaction step,  $E_2$ , is not sensitive to the chain length, then Equation (5.3.28) predicts that the apparent activation energy will decrease with increasing length of the alkane. The temperature invariance of the pseudo-first-order rate constant for cracking of  $\text{C}_{16}$  apparently results from the cancellation of  $E_2$  by  $\Delta H_{\text{ads}}$ . It is also worth mentioning that the magnitude of  $k^*$ , at a constant temperature, will be profoundly affected by carbon chain length through the equilibrium adsorption constant.

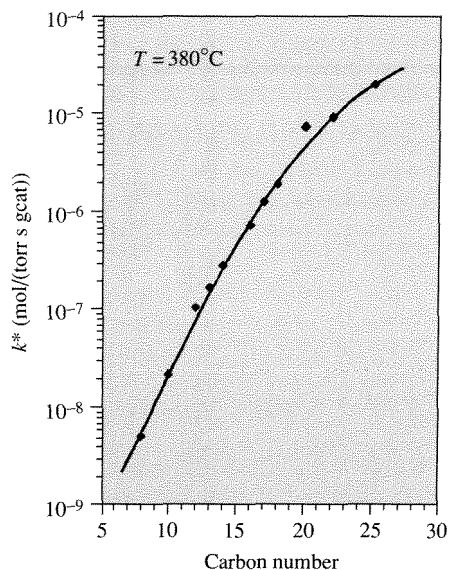


**Figure 5.3.3 |**

The apparent first-order rate constant of n-alkane cracking over ZSM-5 at 380°C. [Reprinted from J. Wei, "Adsorption and Cracking of N-Alkanes over ZSM-5: Negative Activation Energy of Reaction," *Chem. Eng. Sci.*, **51** (1996) 2995, with permission from Elsevier Science.]

Indeed, Figure 5.3.3 illustrates the exponential dependence of  $k^*$  on the size of the alkane molecule. The high enthalpies of adsorption for long chain alkanes means that their surface coverages will far exceed those associated with short chain molecules, which translates into much higher reaction rates.

### VIGNETTE 5.3.1

Zeolites are highly porous, crystalline, aluminosilicates that are widely used as industrial catalysts. In 1756, the Swedish mineralogist A. F. Cronstedt coined the term zeolite, which is derived from the Greek words "zeo," to boil, and "lithos," stone, after he observed that the mineral stilbite gave off steam when heated. Today, it is known that zeolites are constructed from  $\text{TO}_4$  tetrahedral (T = tetrahedral atom, e.g., Si, Al) with each apical oxygen atom shared with an adjacent tetrahedron.

To understand the function of zeolites in a catalytic reaction, it is necessary to first describe the crystal chemistry of their framework. From the valency of silicon it

follows that silicon atoms generally prefer bonds with four neighboring atoms in tetrahedral geometry. If a  $\text{SiO}_4$  entity could be isolated, its formal charge would be  $-4$  since silicon is  $+4$  and each oxygen anion is  $-2$ . However, a defect-free, pure  $\text{SiO}_2$  framework will not contain any charge since an oxygen atom bridges two silicon atoms and shares electron density with each. If aluminum is tetrahedrally coordinated to four oxygen atoms in a framework, the net formal charge is  $-1$  since aluminum carries a  $+3$  valency. When tetrahedra containing silicon and aluminum are connected to form an aluminosilicate framework, there is a negative charge associated with each aluminum atom and it is balanced by a positive ion to give electrical neutrality. Typical cations are alkali metals (e.g.,  $\text{Na}^+$ ,  $\text{K}^+$ ), alkaline earth metals (e.g.,  $\text{Ca}^{2+}$ ,  $\text{Ba}^{2+}$ ), and the proton  $\text{H}^+$ . Figure 5.3.4 illustrates an example of a common cage structure known as sodalite and how it is constructed of silicon, aluminum, and oxygen atoms. Figure 5.3.4 also shows how several different zeolites are comprised of these sodalite cages. Each line in the figure represents a bridging oxygen atom while the intersection locates a silicon or aluminum atom.

Many zeolite structures exist. There are natural zeolites, synthetic analogues of natural zeolites, and synthetic zeolites with no natural counterparts. In all, there are more than 100 structures. Figure 5.3.5 illustrates some typical framework projections containing various rings (pores) of different sizes. Notice that the sizes range from approximately 4 to 12 Å and that the topologies may contain channels and/or cages. What

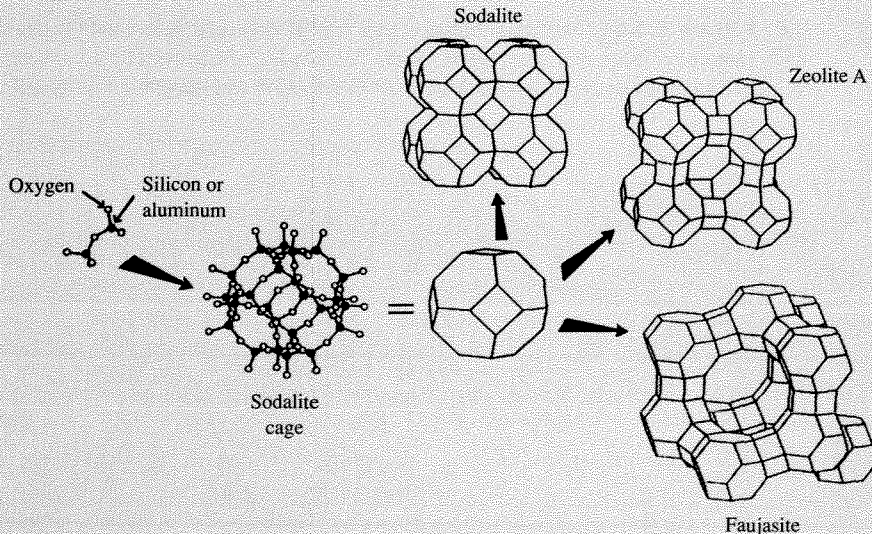


**Figure 5.3.4** | Schematic of zeolite frameworks. The synthetic faujasites are NaX and NaY (difference between NaX and NaY is the ratio of Si to Al: NaX  $\sim 1.1$ , NaY  $\sim 2.4$ ). These constructions do not represent how the materials are synthesized but rather their structural features alone. [Reprinted with permission from M. E. Davis, *Ind. Eng. Chem. Res.*, **30** (1991) 1676. Copyright 1991 American Chemical Society.]

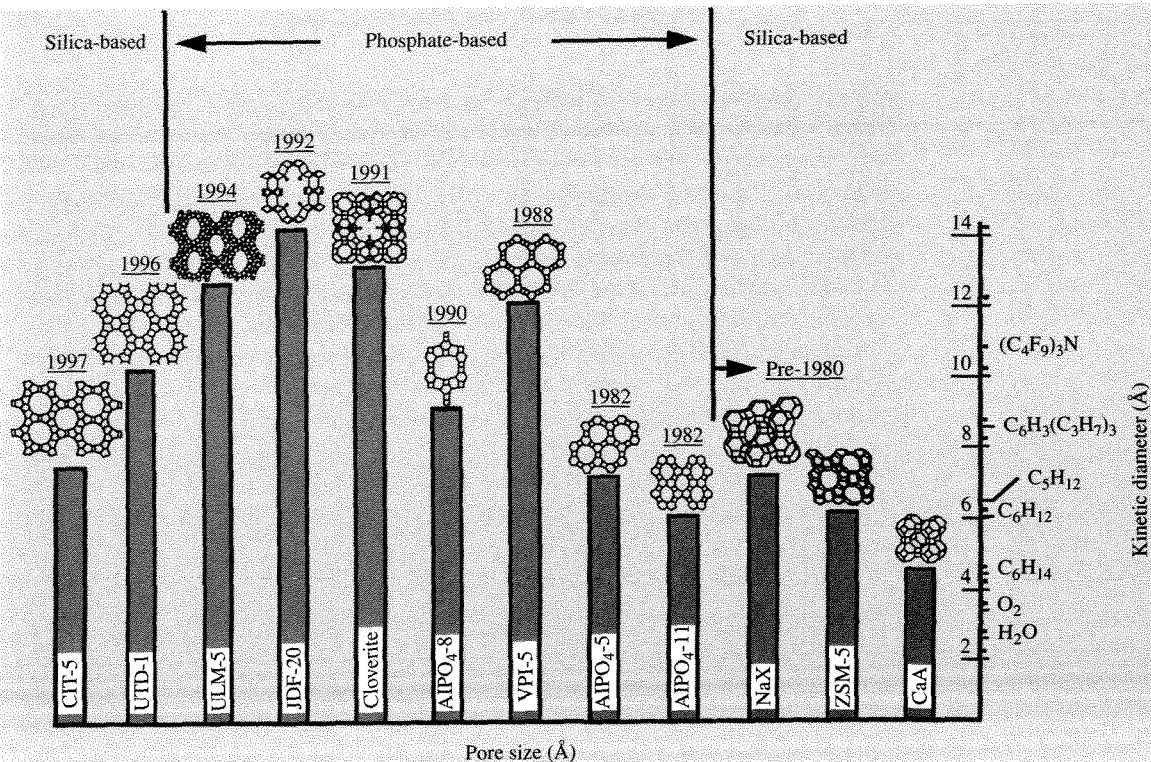


**Figure 5.3.5** | Correlation between pore size of molecular sieves and the diameter of various molecules. [Reprinted from M. E. Davis, "Zeolite-Based Catalysts for Chemicals Synthesis," *Microporous and Mesoporous Mater.*, **21** (1998) 179, with permission of Elsevier Science.]

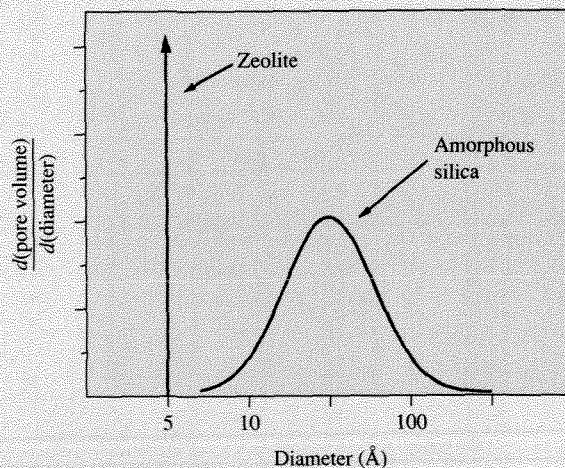


**Figure 5.3.6** | Pore size distribution of zeolite compared to amorphous silica. [Reprinted with permission from M. E. Davis, *Ind. Eng. Chem. Res.*, **30** (1991) 1677. Copyright 1991 American Chemical Society.]

makes zeolites unique is that their pores are uniform in size (see Figure 5.3.6) and that they are in the same size range as small molecules (see Figure 5.3.5). Thus, zeolites are *molecular sieves* since they can discriminate molecules on the basis of size. Molecules smaller than the aperture size are admitted to the crystal interior (adsorbed) while those larger are not.

If the charge balancing cation in a zeolite is  $H^+$ , then the material is a solid acid that can reveal shape selective properties due to the confinement of the acidic proton within the zeolite pore architecture. An example of shape selective acid catalysis is provided in Figure 5.3.7. In this case, normal butanol and isobutanol were dehydrated over CaX and CaA zeolites that contained protons in the pore structure. Both the primary and secondary alcohols were dehydrated on the X zeolite whereas only the primary one reacted on the A zeolite. Since the secondary alcohol is too large to diffuse through the pores of CaA, it cannot reach the active sites within the CaA crystals.

The rate of hexane cracking on the zeolite ZSM-5 has been evaluated as a function of proton content (achieved by varying the Al content in the framework) over

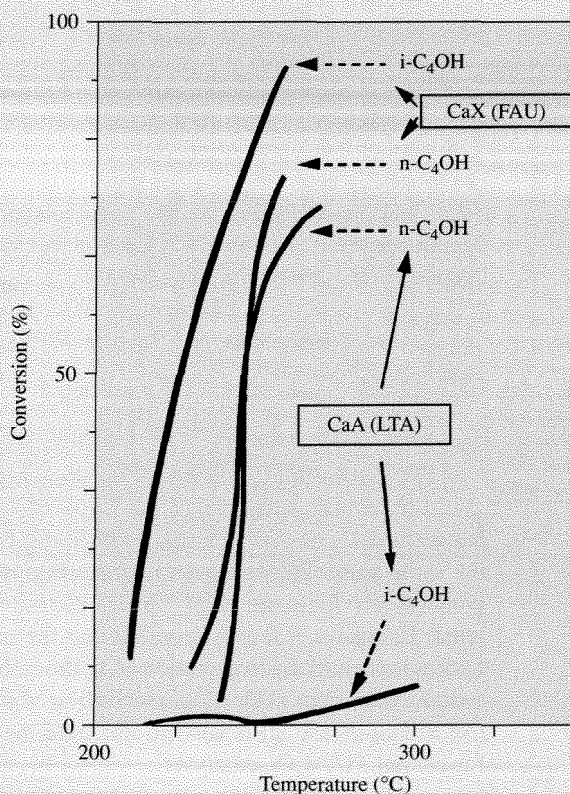


**Figure 5.3.7** | Dehydration of alcohols by zeolites.  
[Reprinted with permission from M. E. Davis, *Ind. Eng. Chem. Res.*, **30** (1991) 1677. Copyright 1991 American Chemical Society.]



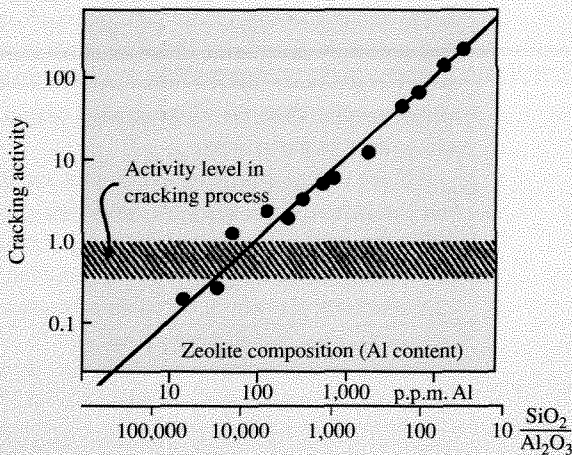
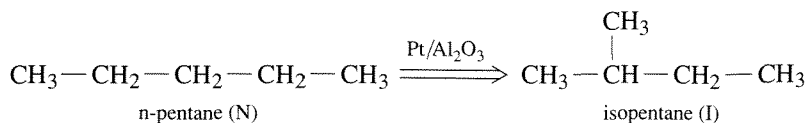


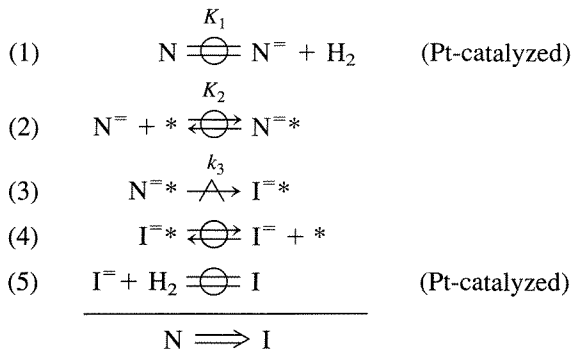
**Figure 5.3.8** | Variation in the hexane cracking activity with aluminum content in ZSM-5. [Reprinted with permission from W. O. Haag, R. M. Lago, and P. B. Weisz, *Nature*, **309** (1984) 589.]

4 orders of magnitude of proton loading (see Figure 5.3.8). Since the rate was found to be strictly proportional to the proton content, these catalytic sites were clearly identical and noninteracting. W. O. Haag concluded that the possibility of synthesizing zeolite catalysts with a well-defined, predetermined number of active sites of uniform activity was certainly without parallel in heterogeneous catalysis (W. O. Haag in "Zeolites and Related Microporous Materials: State of the Art 1994," J. Weitkamp et al., Eds., *Studies in Surface Science and Catalysis*, Vol. 84B, Elsevier Science B.V., 1994, p. 1375).

The discussion to this point has emphasized kinetics of catalytic reactions on a uniform surface where only one type of active site participates in the reaction. Bifunctional catalysts operate by utilizing two different types of catalytic sites on the same solid. For example, hydrocarbon reforming reactions that are used to upgrade motor fuels are catalyzed by platinum particles supported on acidified alumina. Extensive research revealed that the metallic function of  $\text{Pt}/\text{Al}_2\text{O}_3$  catalyzes hydrogenation/dehydrogenation of hydrocarbons, whereas the acidic function of the support facilitates skeletal isomerization of alkenes. The isomerization of *n*-pentane (N) to isopentane (I) is used to illustrate the kinetic sequence associated with a bifunctional  $\text{Pt}/\text{Al}_2\text{O}_3$  catalyst:



The sequence involves dehydrogenation of n-pentane on Pt particles to form intermediate n-pentene ( $N^=$ ), which then migrates to the acidic alumina and reacts to i-pentene ( $I^=$ ) in a rate-determining step. The i-pentene subsequently migrates back to the Pt particles where it is hydrogenated to the product i-pentane. The following sequence describes these processes (where \* represents an acid site on alumina):



Interestingly, the rate is inhibited by dihydrogen even though it does not appear in the stoichiometric equation. The rate is simply:

$$r = r_3 = k_3[N^=*] \quad (5.3.29)$$

The equilibrium relationships for steps 1 and 2 give:

$$[N^*=] = K_2[N^=][*] \quad (5.3.30)$$

$$[N^=] = K_1 \frac{[N]}{[H_2]} \quad (5.3.31)$$

The site balance on alumina (assuming  $N^*=$  is the *mari*, far from equilibrium):

$$[*]_0 = [*] + [N^*=] \quad (5.3.32)$$

and its use along with Equations (5.3.30) and (5.5.31) allow the rate expression for the forward reaction to be written as:

$$r = \frac{K_1 K_2 k_3 [*]_0 [N]}{[H_2] + K_1 K_2 [N]} \quad (5.3.33)$$

Thus, the inhibitory effect of  $H_2$  in pentane isomerization arises from the equilibrated dehydrogenation reaction in step 1 that occurs on the Pt particles.

## 5.4 | Evaluation of Kinetic Parameters

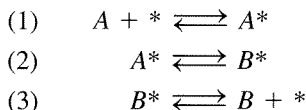
Rate data can be used to postulate a kinetic sequence for a particular catalytic reaction. The general approach is to first propose a sequence of elementary steps consistent with the stoichiometric reaction. A rate expression is derived using the steady-state

approximation together with any other assumptions, like a rate-determining step, a most abundant reaction intermediate, etc. and compared to the rate data. If the functional dependence of the data is similar to the proposed rate expression, then the sequence of elementary steps is considered plausible. Otherwise, the proposed sequence is discarded and an alternative one is proposed.

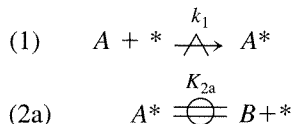
Consider the isomerization of molecule  $A$  far from equilibrium:



that is postulated to occur through the following sequence of elementary steps:



**Case 1.** If the rate of adsorption is rate determining, then the forward rate of reaction can be simplified to two steps:



where step 2a represents the overall equilibrium associated with surface reaction and desorption of product. A rate expression consistent with these assumptions is (derived according to methods described earlier):

$$r = r_1 = k_1[A][*] \quad (5.4.1)$$

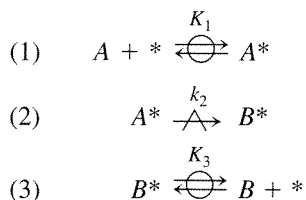
$$K_{2a} = \frac{[A^*]}{[B][*]} \quad (5.4.2)$$

$$[*]_0 = [*] + [A^*] \quad (5.4.3)$$

The equilibrium constant is written such that  $K_{2a}$  is large when  $[A^*]$  is large. Combining Equations (5.4.1–5.4.3) results in the following expression for the forward rate:

$$r = \frac{k_1[*]_0[A]}{1 + K_{2a}[B]} \quad (5.4.4)$$

**Case 2.** If the surface reaction is rate-determining, the following sequence for the forward rate is appropriate:





This particular sequence assumes both  $A^*$  and  $B^*$  are present on the surface in kinetically significant amounts. The rate expression for this case is:

$$r = r_2 = k_2[A^*] \quad (5.4.5)$$

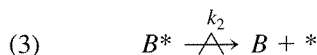
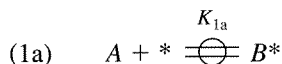
$$K_1 = \frac{[A^*]}{[A][*]} \quad (5.4.6)$$

$$K_3 = \frac{[B^*]}{[B][*]} \quad (5.4.7)$$

$$[*]_0 = [*] + [A^*] + [B^*] \quad (5.4.8)$$

$$r = \frac{k_2[*]_0[A]}{1 + K_1[A] + K_3[B]} \quad (5.4.9)$$

**Case 3.** In this last case, the desorption of product is assumed to be rate determining. Similar to Case 1, two elementary steps are combined into an overall equilibrated reaction:



The expression for the forward rate is derived accordingly:

$$r = r_3 = k_3[B^*] \quad (5.4.10)$$

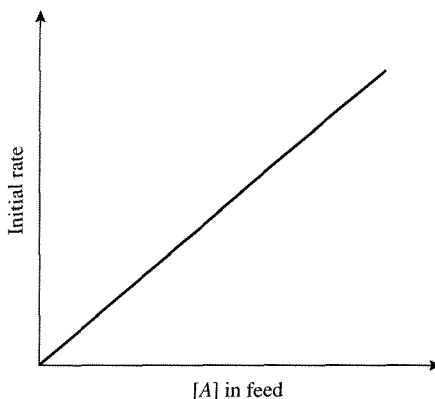
$$K_{1a} = \frac{[B^*]}{[A][*]} \quad (5.4.11)$$

$$[*]_0 = [*] + [B^*] \quad (5.4.12)$$

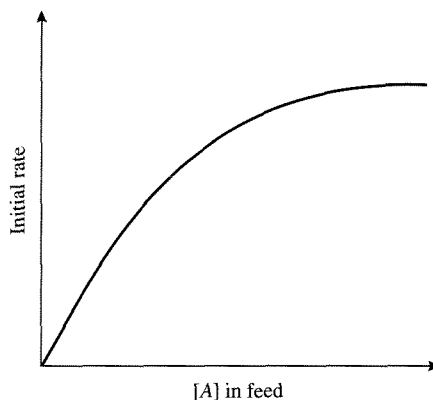
$$r = \frac{k_3 K_{1a} [*]_0 [A]}{1 + K_{1a} [A]} \quad (5.4.13)$$

A common method used to distinguish among the three cases involves the measurement of the initial rate as a function of reactant concentration. Since  $B$  is not present at early reaction times, the initial rate will vary proportionally with the concentration of  $A$  when adsorption of  $A$  is the rate-determining step (Figure 5.4.1).

Similarly, the initial rate behavior is plotted in Figure 5.4.2 for Cases 2 and 3, in which the rate-determining step is either surface reaction or desorption of product. Since the functional form of the rate expression is the same in Cases 2 and 3 when  $B$  is not present, additional experiments are required to distinguish between the two cases. Adding a large excess of product  $B$  to the feed allows for the difference between kinetic mechanisms to be observed. As shown in Figure 5.4.3, the presence of product in the feed does not inhibit the initial rate when desorption of  $B$  is the rate-determining step. If surface reaction of adsorbed  $A$  were the rate-determining

**Figure 5.4.1 |**

Results from Case 1 where adsorption is the rate-determining step.

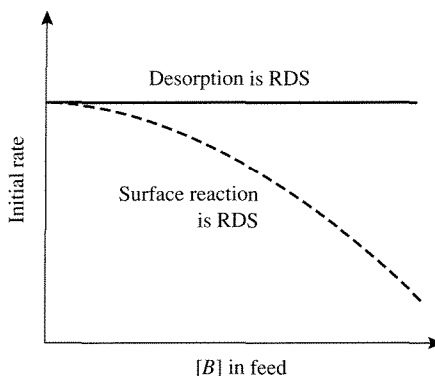
**Figure 5.4.2 |**

Results from Cases 2 and 3 where surface reaction or product desorption is the rate-determining step.

step, then extra  $B$  in the feed effectively competes for surface sites, displaces  $A$  from the catalyst, and lowers the overall rate.

Once a rate expression is found to be consistent with experimental observations, then rate constants and equilibrium constants are obtained from quantitative rate data. One way to arrive at numerical values for the different constants in a Langmuir-Hinshelwood rate expression is to first invert the rate expression. For Case 2, the rate expression:

$$r = \frac{k_2[*]_0[A]}{1 + K_1[A] + K_3[B]} \quad (5.4.14)$$

**Figure 5.4.3 |**

The influence of extra  $B$  on the initial rate (at constant  $[A]$ ) for cases with different rate-determining steps (RDS).

becomes:

$$\frac{1}{r} = \frac{1}{k_2[*]_0[A]} + \frac{K_1[A]}{k_2[*]_0[A]} + \frac{K_2[B]}{k_2[*]_0[A]} \quad (5.4.15)$$

Multiplying by  $[A]$  gives an equation in which the groupings of constants can be calculated by a linear least squares analysis:

$$\frac{[A]}{r} = \frac{1}{k_2[*]_0} + \frac{K_1}{k_2[*]_0}[A] + \frac{K_2}{k_2[*]_0}[B] \quad (5.4.16)$$

The above expression is of the form:

$$y = \bar{\alpha}_1 + \bar{\alpha}_2[A] + \bar{\alpha}_3[B]$$

with

$$y = \frac{[A]}{r}, \quad \bar{\alpha}_1 = \frac{1}{k_2[*]_0}, \quad \bar{\alpha}_2 = \frac{K_1}{k_2[*]_0}, \quad \bar{\alpha}_3 = \frac{K_2}{k_2[*]_0}$$

If an independent measure of  $[*]_0$  is available from chemisorption, the constants  $k_2$ ,  $K_1$ , and  $K_2$  can be obtained from linear regression. It should be noted that many kineticists no longer use the linearized form of the rate equation to obtain rate constants. Inverting the rate expression places greater statistical emphasis on the lowest measured rates in a data set. Since the lowest rates are usually the least precise, a nonlinear least squares analysis of the entire data set using the normal rate expression is *preferred*.

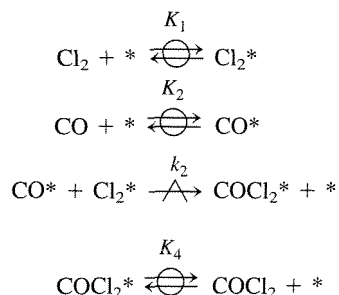
**EXAMPLE 5.4.1**

The reaction  $\text{CO} + \text{Cl}_2 \rightleftharpoons \text{COCl}_2$  has been studied over an activated carbon catalyst. A surface reaction appears to be the rate-determining step. Fashion a rate model consistent with the following data:

Rate ( $\times 10^3 \frac{\text{mol}}{\text{gcat} \cdot \text{h}}$ )	$P_{\text{CO}}$ (atm)	$P_{\text{Cl}_2}$ (atm)	$P_{\text{COCl}_2}$ (atm)
4.41	0.406	0.352	0.226
4.4	0.396	0.363	0.231
2.41	0.310	0.320	0.356
2.45	0.287	0.333	0.376
1.57	0.253	0.218	0.522
3.9	0.610	0.113	0.231
2.0	0.179	0.608	0.206

**■ Answer**

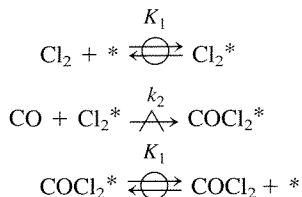
The strategy is to propose a reasonable sequence of steps, derive a rate expression, and then evaluate the kinetic parameters from a regression analysis of the data. As a first attempt at solution, assume both  $\text{Cl}_2$  and  $\text{CO}$  adsorb (nondissociatively) on the catalyst and react to form adsorbed product in a Langmuir-Hinshelwood step. This will be called Case 1. Another possible sequence involves adsorption of  $\text{Cl}_2$  (nondissociatively) followed by reaction with  $\text{CO}$  to form an adsorbed product in a Rideal-Eley step. This scenario will be called Case 2.

**Case 1**

The rate expression derived from the equilibrium relations for steps 1, 2, and 4, assuming all three adsorbed species are present in significant quantities, is:

$$r = \frac{k_3 K_2 K_1 [*]_0 [\text{CO}] [\text{Cl}_2]}{(1 + K_1 [\text{Cl}_2] + K_2 [\text{CO}] + K_4 [\text{COCl}_2])^2}$$

The data fit well the above expression. However, some of the constants (not shown) have negative values and are thus unrealistic. Therefore, Case 1 is discarded.

**Case 2**

Assuming only  $\text{Cl}_2^*$  and  $\text{COCl}_2^*$  are present on the surface, the following rate expression is derived:

$$r = \frac{k_2 K_1 [*]_0 [\text{CO}] [\text{Cl}_2]}{1 + K_1 [\text{Cl}_2] + K_3 [\text{COCl}_2]}$$

Fitting the data to the above equation results in the following rate model:

$$r = \frac{1.642 [\text{CO}] [\text{Cl}_2]}{1 + 124.4 [\text{Cl}_2] + 58.1 [\text{COCl}_2]} \quad \left( \frac{\text{mol}}{\text{gcat-h}} \right)$$

where concentrations are actually partial pressures expressed in atm. Even though all the kinetic parameters are positive and fit the data set reasonably well, this solution is not guaranteed to represent the actual kinetic sequence. Reaction kinetics can be consistent with a mechanism but they cannot prove it. Numerous other models need to be constructed and tested against one another (as illustrated previously in this section) in order to gain confidence in the kinetic model.

Rate constants and equilibrium constants should be checked for thermodynamic consistency if at all possible. For example, the heat of adsorption  $\Delta H_{\text{ads}}$  derived from the temperature dependence of  $K_{\text{ads}}$  should be negative since adsorption reactions are almost always exothermic. Likewise, the entropy change  $\Delta S_{\text{ads}}$  for nondissociative adsorption must be negative since every gas phase molecule loses translational entropy upon adsorption. In fact,  $|\Delta S_{\text{ads}}| < S_g$  (where  $S_g$  is the gas phase entropy) must also be satisfied because a molecule cannot lose more entropy than it originally possessed in the gas phase. A proposed kinetic sequence that produces adsorption rate constants and/or equilibrium constants that do not satisfy these basic principles should be either discarded or considered very suspiciously.

**Exercises for Chapter 5**

1. (a) Calculate the BET surface area per gram of solid for Sample 1 using the full BET equation and the one-point BET equation. Are the values the same? What is the BET constant?
- (b) Calculate the BET surface area per gram of solid for Sample 2 using the full BET equation and the one-point BET equation. Are the values the same? What is the BET constant and how does it compare to the value obtained in (a)?

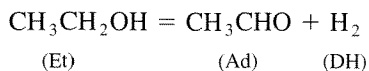
Dinitrogen adsorption data

P/P <sub>0</sub>	Volume adsorbed (cm <sup>3</sup> /g)	
	Sample 1	Sample 2
0.02	23.0	0.15
0.03	25.0	0.23
0.04	26.5	0.32
0.05	27.7	0.38
0.10	31.7	0.56
0.15	34.2	0.65
0.20	36.1	0.73
0.25	37.6	0.81
0.30	39.1	0.89

2. A 0.5 wt. % Pt on silica catalyst gave the data listed below for the sorption of H<sub>2</sub>. Upon completion of Run 1, the system was evacuated and then Run 2 was performed. Find the dispersion and average particle size of the Pt particles. *Hint*: Run 1 measures the total sorption of hydrogen (reversible + irreversible) while Run 2 gives only the reversible hydrogen uptake. Calculate the dispersion based on the chemisorbed (irreversible) hydrogen.

Run 2		Run 1	
Pressure (torr)	H/Pt	Pressure (torr)	H/Pt
10.2	1.09	10.7	1.71
12.9	1.30	14.2	2.01
16.1	1.60	18.2	2.33
20.4	1.93	23.2	2.73
25.2	2.30	28.9	3.17
30.9	2.75	35.9	3.71
37.9	3.30	44.4	4.38
46.5	3.96	55.2	5.22
57.2	4.79	66.2	6.05
68.2	5.64	77.2	6.90
79.2	6.49	88.3	7.72
90.2	7.32	99.3	8.57
101	8.18	110	9.42
112	9.03	121	10.3
123	9.87	132	11.1
134	10.7	143	12.0
145	11.6	154	12.8
156	12.4		

3. A. Peloso et al. [*Can. J. Chem. Eng.*, **57** (1979) 159] investigated the kinetics of the following reaction over a CuO/Cr<sub>2</sub>O<sub>3</sub>/SiO<sub>2</sub> catalyst at temperatures of 225–285°C:



A possible rate expression to describe the data is:

$$r = \frac{k[P_{\text{Et}} - (P_{\text{Ad}}P_{\text{DH}})/K_e]}{[1 + K_{\text{Et}}P_{\text{Et}} + K_{\text{Ad}}P_{\text{Ad}}]^2}$$

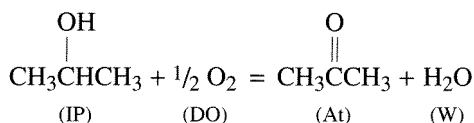
Write a reaction sequence that would give this rate expression.

4. J. Franckaerts and G. F. Froment [*Chem. Eng. Sci.*, **19** (1964) 807] investigated the reaction listed in Exercise 3 over the same temperature range using a CuO/CoO/Cr<sub>2</sub>O<sub>3</sub> catalyst. The rate expression obtained in this work was of the form:

$$r = \frac{k[P_{\text{Et}} - (P_{\text{Ad}}P_{\text{DH}})/K_e]}{[1 + K_{\text{Et}}P_{\text{Et}} + K_{\text{Ad}}P_{\text{Ad}} + K_{\text{DH}}P_{\text{DH}}]^2}$$

Write a reaction sequence that gives a rate expression of this form. What is different from the sequence used in Exercise 3?

5. The following oxidation occurs over a solid catalyst:

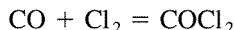


If acetone cannot adsorb and the rate of surface reaction between adsorbed isopropanol and adsorbed oxygen is the rate-determining step, a rate expression of the form:

$$r = \frac{k[\text{IP}][\text{DO}]^{\frac{1}{2}}}{(1 + K_1[\text{IP}] + K_2[\text{W}])(1 + K_3[\text{DO}]^{\frac{1}{2}})}$$

can be obtained from what reaction sequence?

6. For the reaction:



the rate expression given below can be obtained:

$$r = \frac{kP_{\text{CO}}P_{\text{Cl}_2}}{[1 + K_1P_{\text{Cl}_2} + K_2P_{\text{COCl}_2}]^2}$$

What does the exponent on the denominator imply and what does the lack of a  $K_3P_{\text{CO}}$  term in the denominator suggest?

7. For the reaction of A to form B over a solid catalyst, the reaction rate has the form:

$$r = \frac{kK_A P_A}{(1 + K_A P_A + K_B P_B)^2}$$

However, there is a large excess of inert in the reactant stream that is known to readily adsorb on the catalyst surface. How will this affect the reaction order with respect to A?

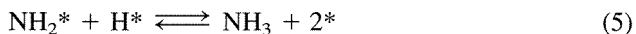
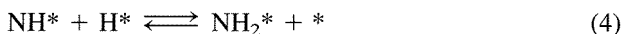
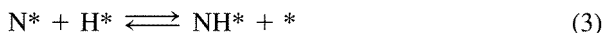
8. G. Thodor and C. F. Stutzman [*Ind. Eng. Chem.*, **50** (1958) 413] investigated the following reaction over a zirconium oxide-silica gel catalyst in the presence of methane:



If the equilibrium constant for the reaction is 35 at reaction conditions, find a reaction rate expression that describes the following data:

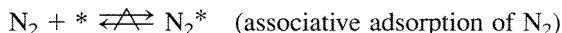
$r \times 10^4 \text{ (mol/h/(lb cat))}$	Partial pressure (atm)			
	$\text{CH}_4$	$\text{C}_2\text{H}_4$	$\text{HCl}$	$\text{C}_2\text{H}_5\text{Cl}$
2.66	7.005	0.300	0.370	0.149
2.61	7.090	0.416	0.215	0.102
2.41	7.001	0.343	0.289	0.181
2.54	9.889	0.511	0.489	0.334
2.64	10.169	0.420	0.460	0.175
2.15	8.001	0.350	0.250	0.150
2.04	9.210	0.375	0.275	0.163
2.36	7.850	0.400	0.300	0.208
2.38	10.010	0.470	0.400	0.256
2.80	8.503	0.500	0.425	0.272

9. Ammonia synthesis is thought to take place on an iron catalyst according to the following sequence:



Obviously, step 2 must occur three times for every occurrence of step 1, and steps 3–5 each occur twice, to give the overall reaction of  $\text{N}_2 + 3\text{H}_2 = 2\text{NH}_3$ . Experimental evidence suggests that step 1 is the rate-determining step, meaning that all of the other steps can be represented by one pseudo-equilibrated overall reaction. Other independent evidence shows that nitrogen is the only surface species with any significant concentration on the surface (most abundant reaction intermediate). Thus,  $[*]_0 = [*] + [\text{N}^*]$ . Equation (5.3.7) gives the rate expression consistent with the above assumptions.

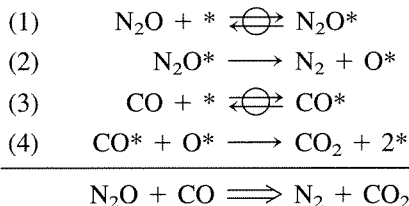
(a) Now, assume that the rate-determining step is actually:





with  $N_2^*$  being the most abundant reaction intermediate. Derive the rate expression for the reversible formation of ammonia.

- (b) Can the rate expression derived for part (a) and the one given in Equation (5.3.7) be discriminated through experimentation?
10. Nitrous oxide reacts with carbon monoxide in the presence of a ceria-promoted rhodium catalyst to form dinitrogen and carbon dioxide. One plausible sequence for the reaction is given below:



- (a) Assume that the surface coverage of oxygen atoms is very small to derive a rate expression of the following form:

$$r = \frac{K_1 P_{N_2O}}{1 + K_2 P_{N_2O} + K_3 P_{CO}}$$

where the  $K$ 's are collections of appropriate constants. Do not assume a rate-determining step.

- (b) The rate expression in part (a) can be rearranged into a linear form with respect to the reactants. Use linear regression with the data in the following table to evaluate the kinetic parameters  $K_1$ ,  $K_2$ , and  $K_3$ .

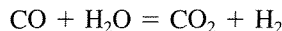
Rates of  $N_2O + CO$  reaction at 543 K

$P_{CO}$ (torr)	$P_{N_2O}$ (torr)	Turnover rate ( $s^{-1}$ )
30.4	7.6	0.00503
30.4	15.2	0.00906
30.4	30.4	0.0184
30.4	45.6	0.0227
30.4	76	0.0361
7.6	30.4	0.0386
15.2	30.4	0.0239
45.6	30.4	0.0117
76	30.4	0.00777

Source: J. H. Holles, M. A. Switzer, and R. J. Davis, *J. Catal.*, **190** (2000) 247.

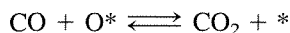
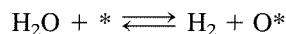
- (c) Use nonlinear regression with the data in part (b) to obtain the kinetic parameters. How do the answers compare?
- (d) Which species,  $N_2O$  or  $CO$ , is present on the surface in greater amount?

11. The reaction of carbon monoxide with steam to produce carbon dioxide and dihydrogen is called the water gas shift (WGS) reaction and is an important process in the production of dihydrogen, ammonia, and other bulk chemicals. The overall reaction is shown below:



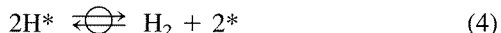
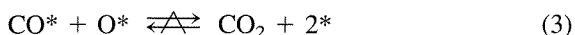
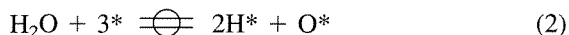
Iron-based solids that operate in the temperature range of 360 to 530°C catalyze the WGS reaction.

- (a) One possible sequence is of the Rideal-Eley type that involves oxidation and reduction of the catalyst surface. This can be represented by the following steps:



Derive a rate expression.

- (b) Another possible sequence for the WGS reaction is of the Langmuir-Hinshelwood type that involves reaction of adsorbed surface species. For the following steps:

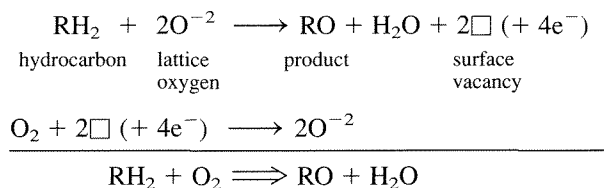


derive the rate expression. (Notice that step 2 is an overall equilibrated reaction.) Do not assume that one species is the most abundant reaction intermediate.

12. For the hydrogenation of propionaldehyde ( $\text{CH}_3\text{CH}_2\text{CHO}$ ) to propanol ( $\text{CH}_3\text{CH}_2\text{CH}_2\text{OH}$ ) over a supported nickel catalyst, assume that the rate-limiting step is the reversible chemisorption of propionaldehyde and that dihydrogen adsorbs dissociatively on the nickel surface.
- (a) Provide a reasonable sequence of reaction steps that is consistent with the overall reaction.
- (b) Derive a rate expression for the rate of consumption of propionaldehyde. At this point, do not assume a single *mari*.
- (c) Under what conditions would the rate expression reduce to the experimentally observed function (where *prop* corresponds to propionaldehyde, and *P* represents partial pressure):

$$r = \frac{kP_{\text{prop}}}{P_{\text{H}_2}^{0.5}}$$

13. Some of the oxides of vanadium and molybdenum catalyze the selective oxidation of hydrocarbons to produce valuable chemical intermediates. In a reaction path proposed by Mars and van Krevelen (see Section 10.5), the hydrocarbon first reduces the surface of the metal oxide catalyst by reaction with lattice oxygen atoms. The resulting surface vacancies are subsequently re-oxidized by gaseous  $O_2$ . The elementary steps of this process are shown below. Electrons are added to the sequence to illustrate the redox nature of this reaction.



Derive a rate expression consistent with the above sequence. For this problem, assume that the vacancies do not migrate on the surface. Thus,  $2\text{O}^{-2}$  and  $2\square$  can be considered as a single occupied and a single unoccupied surface site, respectively. Show that the expression can be transformed into the following form:

$$\frac{1}{r} = \frac{1}{K_1[\text{RH}_2]} + \frac{1}{K_2[\text{O}_2]}$$

where the  $K$ 's are collections of appropriate constants.